1964

Photoconductivity of Non-Ionic Crystalline Organic Substances.

Leo Villaraiz Azarraga
Louisiana State University and Agricultural & Mechanical College

PHOTOCONDUCTIVITY OF NON-IONIC CRYSTALLINE ORGANIC SUBSTANCES

A Dissertation

Submitted to the Graduate Faculty of the
Louisiana State University and
Agricultural and Mechanical College
in partial fulfillment of the
requirements for the degree of
Doctor of Philosophy

in

The Department of Chemistry

by
Leo Villaraiz Azarraga
B.S., University of the Philippines, 1956
August, 1964

ACKNOWLEDGMENT

The author wishes to express his gratitude to Dr. Sean P. McGlynn whose advice and sincere encouragement have guided and made possible the completion of this work. Special thanks are due to Dr. R. Raman who has been generous with both his time and effort in the preparation of the section on transient methods and to S. D. Thompson, T. Azumi, J. Harris and A. T. Armstrong who in one way or another have rendered valuable assistance during the course of this research.

TABLE OF CONTENTS

LIST OF TABLES

LIST OF FIGURES

ABSTRACT

The photocurrent in organic molecular crystals was studied as a function of voltage, temperature, intensity of illumination, wavelength of excitation, etc. in order to understand the processes involved in photoconduction. The compounds chosen were biphenyl, m-terphenyl, p-terphenyl, p-quarterphenyl, anthracene, rubrene and tetraphenylbutadiene. The crystals were grown from the melt between two semi-transparent SnO_2-coated quartz plates. Electrical contact was made through the SnO_2 film.

The current-voltage characteristics are generally super-linear. The variation of the photocurrent with light intensity is sublinear, linear or super-linear, depending upon the mode of illumination and the applied electric field. The photoconduction action spectrum is generally shifted toward the red and contains more structure than the corresponding absorption spectrum of the compound. Conductivity glow curve experiments yield values of 0.39 ev. and 0.60 ev. for trap depths in m-terphenyl and anthracene crystals respectively. The analyses of the transient photocurrent yield values of mobility of charge carriers, surface trap depths, thermal dependence of mobility, thermal dependence of carrier population and quantum efficiency.

It is indicated that in the polyphenyl series, the increase in the intermolecular interaction enhances the photoconductivity of the compounds in the series; the effect of surface recombination may not be neglected in the kinetics of photoconduction and the photogenerative process at the surface may be biphotonic. It also appears that the charge carriers are scattered mainly by acoustical phonons.

CHAPTER I

INTRODUCTION

A solid under the influence of an applied electric field may show an appreciable increase in electrical conductivity when irradiated with light of suitable wavelengths. Such an enhancement of electrical conduction by optical excitation is termed photoconduction, a phenomenon which may be observed in organic and inorganic solids. Among organic substances, those having extensive π-electron systems are apparently the most photosensitive. It seems, therefore, natural to search for a connection between photoconduction and the excitation of the π-electrons of the aromatic hydrocarbons.

Our previous work indicated that excitation of the molecule to the first singlet excited state is kinetically more important than the excitation of the molecule to its triplet state insofar as the process of charge carrier generation by optical excitation is concerned.[1] It also seemed that an increase in inter-molecular interaction might lead to higher photoconductivity.

With this in mind, it was decided to study the photoconductive properties of a series of compounds of similar molecular structures; the polyphenyl series immediately suggested itself, and was chosen. A number of other aromatic hydrocarbons (i. e., tetraphenylbutadiene, rubrene and anthracene) which were known to be of high photosensitivity were also investigated.

---

[1] M. Kleinerman, L. Azarraga and S. P. McGlynn, J. Chem. Phys., 37, 1825 (1962).

Although the main purpose of the work was directed toward understanding photoconductive processes, some study of the semiconductive properties of these compounds was indicated and was made. Most of the results were obtained from the study of the photocurrent when a D. C. voltage was applied across the crystal while the crystal was under constant ambient illumination (Steady State Method). There are, however, important parameters, such as the lifetime, τ, and the mobility, μ, of the charge carriers, which are not obtainable directly from steady state measurement of conductivity. A pulse technique known as the crystal conductivity counter method was consequently employed to study the characteristics of the transient photocurrents. Unfortunately, sensitivity limitations confined the transient studies to the more photosensitive materials, viz., anthracene and tetraphenylbutadiene.

CHAPTER II

EXPERIMENTAL

The general descriptions of the experimental techniques used in this research are given below. Details of a particular experimental method will be described in conjunction with the discussion of the results thereby obtained.

A. Chemicals

The compounds used in this work were carefully purified. The methods used were recrystallization, vacuum sublimation and zone refining. Zone refining was extensively employed for the final stage of purification. The material was considered pure when no further significant change in the dark current was observed after successive purifications. This seemed to be a better criterion for purity than melting point tests or absorption spectroscopy. The relative merits of this criterion were particularly evident in the cases of biphenyl and m-terphenyl. After several recrystallizations from absolute ethanol, the purified materials were allowed to dry. The melting point and the absorption spectra showed that the materials were "pure." Yet the very high dark conductivity masked the photocurrent completely. After successive zone refinings, which did not further affect melting points or absorption spectra, the dark current was reduced and the observable photocurrent was increased. A faster response to illumination was also observed. The presence of relatively large dark currents and the reduction of these dark currents upon further zone refining indicates the presence of impurities and illustrates the effectiveness of the zone refining method of purification. The impurities were probably trapped in the host crystal during the process of recrystallization and may have consisted of ethanol and water molecules occluded in the crystal. The dark currents observed for the "impure" (i. e., recrystallized) materials were of the order of 10^{-9} to 10^{-8} amperes/cm^2 in an electric field of approximately 10^3 V. cm^{-1}. The dark current for the

"pure" (i. e., extensively zone refined) material was usually less than 10^{-12} amperes/cm^2 at approximately the same electric field. Consequently, the word "pure" in this work has a connotation synonymous with the term "extensively zone refined," the latter being preferred to the former for descriptive accuracy. The methods of purification and the sources of the various compounds follow:

Biphenyl: Matheson, Coleman and Bell, Inc., East Rutherford, N. J.; recrystallized three times from absolute ethanol, and extensively zone refined.

m-Terphenyl: Matheson, Coleman and Bell, Inc., East Rutherford, N. J.; recrystallized from absolute ethanol three times; extensively zone refined.

p-Terphenyl: Pilot Chemicals, Inc., Watertown 72, Mass.; extensively zone refined.

p-Quarterphenyl: Pilot Chemicals, Inc., Watertown 72, Mass.; extensively zone refined.

Anthracene: (1) Pilot Chemicals, Inc., Watertown 72, Mass.; extensively zone refined.

(2) Eastman Organic Chemicals, Rochester 3, N. Y.; Eastman H480.

1,1',4,4' - Tetraphenylbutadiene - 1,3: Pilot Chemicals, Inc., Watertown 72, Mass.; extensively zone refined.

5,6,11,12 - Tetraphenylnaphthacene (Rubrene): K and K Laboratories, Inc., Jamaica 33, New York; vacuum sublimed twice.

B. Preparation of SnO_2-Quartz Electrode Systems

Optical grade quartz plates 1 x 1 x 1/16 inches obtained from Amersil Quartz Division, Hillside, New Jersey were coated with a transparent film of SnO_2. Prior to the coating process, the quartz squares were cleaned in a hot, concentrated solution of nitric and sulfuric acids. The plates were then washed free of acids and rinsed thoroughly with distilled water. Thereafter, they were placed in an oven and dried at 150°C.

Suitable electrode geometry was drawn with india ink pen or with a ball point pen on the quartz surface. The area to be coated was maintained at 1.5 cm^2. The area not to be coated was painted with a "dag", a dispersion of graphite in alcohol. The plate was heated to around 600°C in a Marshall furnace and a stream of $SnCl_2$ vapor mixed with air was directed normal to the surface of the quartz squares. A uniform and transparent film of SnO_2 was formed on the exposed surface. The transparency of the films vary with the length of time of exposure to the vapor. Films with resistances of a few thousand ohms were found to be satisfactorily transparent. The films transmitted light uniformly from 650 to 310 mμ. Light absorption was observed to begin at 310 mμ. After the coating process, most of the masking paint was removed by rubbing with tissue paper soaked in ethanol. The plates were then boiled in a solution of concentrated nitric and sulfuric acids to remove the remaining dag. Thereafter, they were thoroughly washed free from acids in a stream of distilled water. The cleansed SnO_2-Quartz electrodes were stored in an oven at 150°C until needed.

C. Preparation of the "Sandwich" Conductivity Cell

The cell arrangement was essentially identical to that used by Northrop and Simpson.[1] The purified material was placed between two SnO_2-Quartz electrodes separated by a teflon spacer. This spacer was 1 mil or 1/2 mil thick, and had been washed previously in acetone, absolute alcohol and distilled water in that order and dried at 110°C. The cell was placed between two brass plates and the whole assembly was placed in a "Hevi Duty" furnace which had been preheated to 5°C above the melting point of the compounds in question. A brass weight was placed on top of the cell assembly to squeeze out the excess melt. The molten material was allowed to cool slowly. The cooling rate used was that of the furnace itself. About 9 to 10 hours were required to

---

[1] D. C. Northrop and O. Simpson, Proc. Roy. Soc., 244A, 377 (1958).

cool the cell to room temperature. The conductivity cells were usually made in air; some cells were prepared under nitrogen athmosphere. No significant difference in the conductivities was observed between the cells prepared under the two different athmospheres. Variation in the crystallinity of the material did cause a large difference in electrical properties. Generally, glassy type crystals, typical of those obtained from p-terphenyl and p-quarterphenyl, and oriented needle-like crystals typical of m-terphenyl cells, showed lower photocurrents, slower response to illumination and greater super-linearity of current-voltage characteristics than the corresponding cells of better crystal quality. Selection of cells was based on uniformity of extinction under crossed polaroid. For photoconductivity measurements, the region of uniform extinction was isolated by blocking out the rest of the area with dag dispersion or black electrical tape. Electrical contact with the crystal was made through the SnO_2 film.

D. Steady State Method

The cell was connected in series with a stable power supply and the Keithley 610A micromicroammeter. The power supply was made of a parallel combination of dry cell batteries. A Brown-Honeywell recorder connected to the output of the micromicroammeter recorded the steady state current. For the study of the photocurrent, a stable source of exciting radiation was obtained from a D. C. operated, quartz-jacketed G. E. A-H6 lamp.

D-1. Current-Voltage Characteristics

The current-voltage characteristics were studied mostly at room temperature. Only one current-voltage characteristic was determined in the neighborhood of liquid nitrogen temperatures; the cell material was anthracene. The power supplies were battery packs. Individual battery packs were made from suitable combinations of dry cell batteries. A power supply made of a parallel combination of eight 300-volt batteries

and a 100,000 ohm potentiometer was also used. This power supply was limited to short periods of operation because its stability was adversely affected by the relatively large current that drained from the batteries through the potentiometer.

D-2. Dependence of Photocurrent on Light Intensity

The dependence of photocurrent on incident light intensity was studied using both poly- and monochromatic light. Neutral optical density screens calibrated with Cary model 14R spectrophotometer were used to vary the light intensity.

D-3. Photoconductivity Action Spectrum

The dependence of the photocurrent on the wavelength of incident light was studied at room temperature using the Bausch and Lomb grating monochromator. Photocurrents were corrected for unequal incident light intensity by assuming that the equation:

$$J_{p_\lambda} = \xi I_\lambda \tag{1}$$

was valid for all wavelengths. J_{p_λ} was the photocurrent observed for the incident light of wavelength λ and intensity I_λ, and ξ is a proportionality constant directly related to the quantum efficiency of charge carrier production. The correction factor was calculated by normalizing the intensities of the various wavelength bands of the light output of the A-H6 lamp, whence the corrected photocurrent was given by

$$J_{p_{\lambda corr.}} = J_{p_\lambda} \cdot 1/I_\lambda = \xi \tag{2}$$

The values for I_λ were taken from the published data for the spectral distribution of the A-H6 and B-H6 light sources by the General Electric Company.

D-4. Measurement of Activation Energies

The measurement of dark currents and photocurrents at various temperatures was carried out using conduction chambers designed to maintain the conductivity cells at different ambient temperatures.

The temperature of the conduction chamber which was used for making measurements at low temperatures was controlled by a regulated flow of nitrogen vapor coming from a liquid nitrogen reservoir. The temperature inside the conduction chamber was measured with a Rosemont Engr. Co. LH_2 resistance-type temperature transducer. The transducer was calibrated at liquid nitrogen, solid carbon dioxide and ice water temperatures. The conduction chamber was made of an aluminum cylinder. At one end of the cylinder was placed a quartz window which permitted direct illumination of the crystal conductivity cell; this window was maintained fog-free by a strong jet of dry nitrogen gas. Thermal insulation of the chamber was provided by a prefabricated asbestos pipe insulation. The whole assembly was enclosed in a lucite plastic box which acted simultaneously as a dry box and as a secondary insulation by preventing the too-rapid escape of cool nitrogen gas from the conduction chamber. When temperatures above room temperature were desired, another conduction chamber built inside a Fisher Scientific oven was used. A quartz window placed in the oven door permitted direct illumination of the conductivity cell.

The activation energies were evaluated from the slopes of the lines obtained when the logarithm of the current was plotted against the reciprocal of absolute temperature.

E. Measurement of Trap Depths from Thermally Stimulated Currents

The electrical analogue of the thermoluminescent glow curves which have been used by several authors to study trapping of charge carriers in several different materials is what we shall refer to as

the conductivity glow curve.[2-5] When a crystal is irradiated at low temperatures so that the trapping centers are filled and then the crystal is heated in the dark, a transient current due to the thermally stimulated emptying of the traps is obtained.

Randall and Wilkins derived a first-order equation for the glow curve from which the relationship between the trap depth, E_t, and the temperature, T_{max}, at the glow peak may be obtained.[6] Their equation is:

$$E_t = RT_{max} [1 + f(\nu,\beta)] \log \nu \qquad (3)$$

where R is the ideal gas constant, T_{max} is in degrees absolute and $f(\nu,\beta)$ is a function of the attempt-to-escape frequency, ν, and the rate of heating, β. Grossweiner, upon introducing a very reasonable approximation in the equation for the first order glow curve derived by Randall and Wilkins, showed that the trap depths may be calculated from the values of T_{max} and the temperature $T_{1/2}$ at which the low temperature side of the conductivity glow curve attains one half its maximum intensity.[7] The relationship according to Grossweiner is:

$$E_t = 1.51\ k\ T_{max}\ T_{1/2}\ /(T_{max} - T_{1/2}) \qquad (4)$$

where E_t is expressed in electron volts (ev), k is the Boltzmann constant and the T's are absolute temperatures. The above equation was used to calculate the trap depths from the conductivity glow curves of m-terphenyl and anthracene.

---

[2] R. H. Bube, Phys. Rev., 106, 703 (1957).

[3] R. J. Van Heyningen and F. C. Brown, Phys. Rev., 111, 462 (1958).

[4] G. F. Garlick and M. H. F. Wilkins, Proc. Roy. Soc., 184A, 408 (1945).

[5] J. T. Randall and M. H. F. Wilkins, Proc. Roy. Soc., 184A, 347 (1945).

[6] Ibid., p. 366.

[7] L. I. Grossweiner, J. Appl. Phys., 24, 1306 (1953).

To obtain the conductivity glow curves for the compounds previously mentioned, the sandwich conductivity cell was slowly cooled down to near liquid nitrogen temperatures while a D. C. voltage was applied across the cell. The cell was then irradiated with polychromatic light from the A-H6 for a period of approximately five minutes. After the illumination was terminated, nitrogen gas at room temperature was circulated in the conduction chamber in order to warm the cell at a reasonably rapid rate without introducing overly large thermal strains which invariably caused the sandwich cell to break up. The heating rate was not uniform over the temperature range from 100° to 280°K. Between 100 and 200°K the rate was approximately 10° per minute and above 200°K it was about 0.5° per minute. The transient dark current was followed with the 610 electrometer and the Brown-Honeywell recorder.

F. Absorption and Fluorescence Spectra

The absorption and fluorescence spectra were obtained from solutions in fluorometric grade solvents. The Cary model 14R spectrophotometer was used to obtain the absorption spectra at room temperature. Fluorescence and phosphorescence spectra were taken with the Aminco-Kiers Spectrophosphorimeter at liquid nitrogen temperature.

G. The Transient Photoconductivity Method

(See Chapter IV)

CHAPTER III

RESULTS AND DISCUSSION OF STEADY STATE PHOTO- AND SEMICONDUCTION

A. Current-Voltage Characteristics

m-Terphenyl: The current-voltage characteristics of a 49 micron-thick crystal of m-terphenyl are shown in Fig. 1. Curve 1 was taken without illuminating the crystal. It is seen that the dark current varies as $V^{0.4}$ below 150 volts and as V^2 between 200 and 600 volts. The slow rise of the dark current with voltage in the lower voltage range may indicate a tendency of the current to saturate. This would be the case if the electric field, $E = V/d$, is large enough such that the range or Schubweg, of the charge carriers, $\omega = E\mu\tau$, becomes comparable to, if not larger than, the thickness, d, of the crystal. This deduction is based on another form of Hecht's equation given by Mott and Gurney,

$$Y = (\omega/d)\ [1-(\omega/d)(1-e^{-d/\omega})] \qquad (5)$$

which gives the current-voltage relationship when the electric field in the crystal is uniform and the charge carriers are generated uniformly throughout the crystal bulk.[1] In Eq. (5) Y is the ratio of the charge released in the crystal to the charge passing through the external circuit. Eq. (5) predicts that at relatively low electric fields the current will rise approximately linearly with voltage and will tend to saturate when the applied electric field is high enough such that $\omega \gtrsim d$. When the crystal is operating at saturated conditions, the rate at which the charge carriers are extracted from the crystal is equal to the rate at which they are generated in the crystal. An approach to this condition seems to prevail in the lower voltage range of curve 1.

---

[1] N. F. Mott and R. W. Gurney, "Electronic Processes in Ionic Crystals", Clarendon Press, Oxford (1948), p. 122.

Fig. 1. Current-Voltage Characteristics: m-Terphenyl

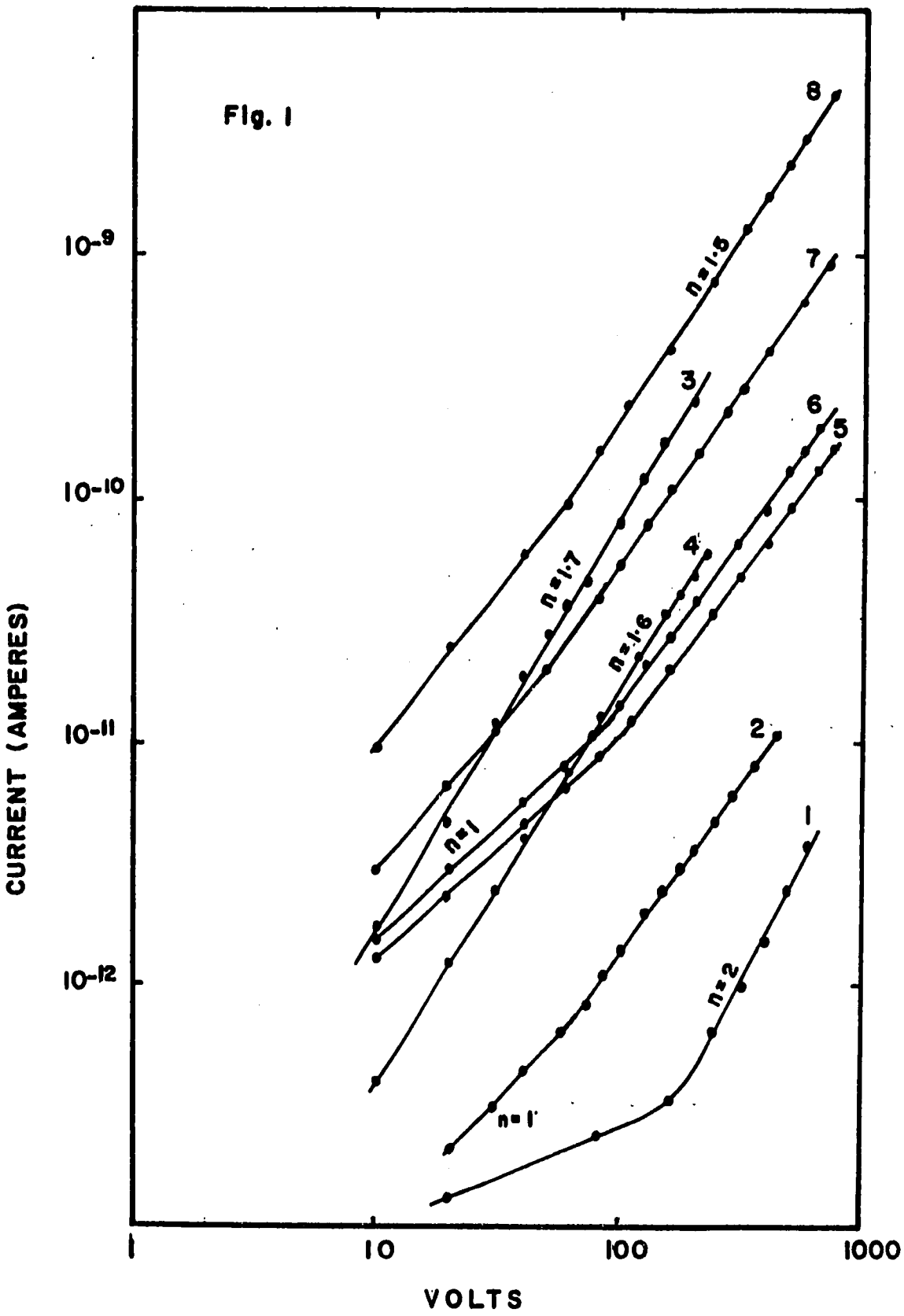
Fig. 1
CURRENT (AMPERES)
10-9
10-10
10-11
10-12
1
10
100
1000
VOLTS
8
7
6
5
4
3
2
1
n=1.8
n=1.7
n=1.6
n=1
n=2
n=1

At voltages above 150 volts the current increases as the square of the voltage. This transition to a V^2 dependence probably takes place for the following reason: Above 150 volts the electric field is large enough so that the charge carriers are swept out of the crystal, those of one polarity being swept out more rapidly than those of opposite polarity. Consequently, a space charge is set up in the crystal and injection of charge carriers from the electrodes takes place to compensate for this space charge. The V^2 portion of curve 1 is then due to a space charge limited current, J, and is predicted by the well known equation for space charge-limited-currents (SCLC) in insulators with shallow traps:[2]

$$J = 10^{-13} [V^2(\mu\theta)\epsilon/d^3] \text{ amperes cm}^{-2} \qquad (6)$$

$$\theta = (N_v/N_t)\, e^{-E_t/kT} \qquad (7)$$

where θ is the fraction of the free space charge, μ is the charge carrier mobility, ϵ is the dielectric constant, N_v is the density of states in the valence band, N_t is the density of trapping states at an energy E_t above the valence band, k is the Boltzmann constant and T is the absolute temperature. The fraction of the free space charge may be calculated from the V^2 region of the curve and the value of hole mobility, $\mu_+ = 10^{-5}$ $cm^2\ V^{-1}\ sec^{-1}$ from Table IX. The dark current at V = 400 volts is 1.65×10^{-11} amp./1.5 cm^2 or approximately 1×10^{-11} amp. cm^{-2}. Using $\epsilon \sim 3$ and $d = 5 \times 10^{-3}$ cm, the value for θ is 2.6×10^{-6}. The trap depth which was found for the main glow peak of the conductivity glow curve shown in Fig. 2 is $E_t = 0.39$ ev. From Eq. (7) the trapping state density may be calculated taking $N_v = 2.4 \times 10^{19}$ at room temperature[3], kT = 1/40 ev. and the values obtained for θ and E_t. The value for N_t turns out to be 1.8×10^{18} cm^{-3}. From the temperature at the maximum of the conduct-

---

[2] A. Rose, Phys. Rev., 97, 1538 (1955).

[3] P. Mark and W. Helfrich, J. Appl. Phys., 33, 205 (1962).

Fig. 2. Conductivity Glow-Curve: m-Terphenyl

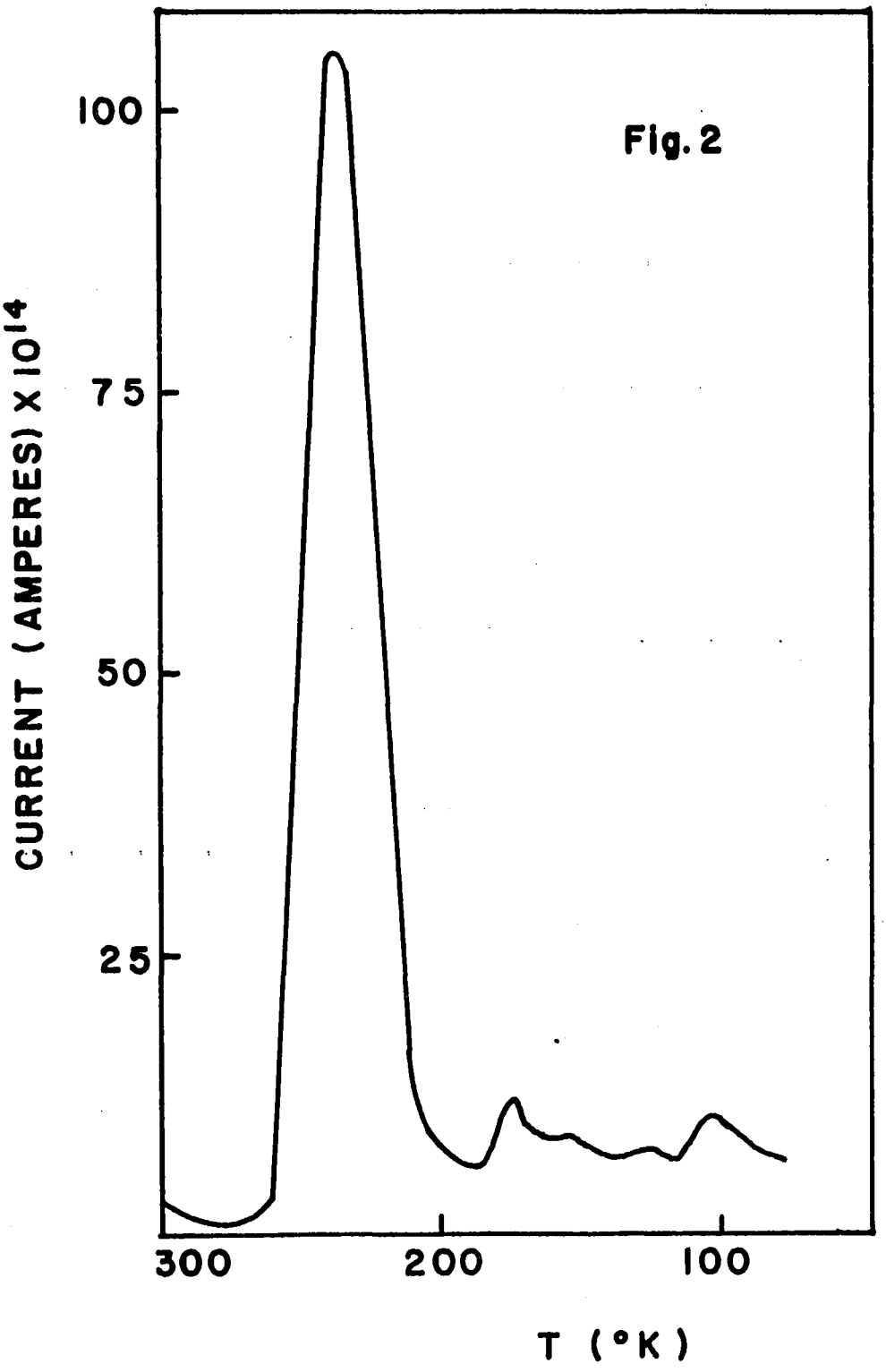
Fig. 2
100
75
50
25
CURRENT (AMPERES) X 10^14
300
200
100
T (°K)

ivity glow curve, $T_{max} = 240^{o}K$, and E_t, the escape frequency from the traps, ν, may be obtained by approximating Eq. (3) as $E_t = kT_{max} \log \nu$ since $f(\nu,\beta)<1$. The escape frequency is found to be 3.6×10^{8} sec^{-1}. The escape frequency is related to the effective density of states in the valence band by $\nu/\sigma_t v_{th} = N_v$ from which the trapping cross-section, σ_t, may be calculated.[4] Assuming that the velocity of the charge carriers at room temperature, v_{th}, is of the order of 10^{7} cm sec^{-1}, the value of σ_t is found to be 1.5×10^{-18} cm^2. The charge carriers spend on the average a time, $\tau_o = (N_t \sigma_t v_{th})^{-1}$, in the conducting states. The values of N_t, σ_t, and v_{th} yield approximately 4×10^{-8} sec for τ_o. Since the experimentally determined value of μ is rather small and the density of trapping states is quite large, it seems reasonable to conclude that the mobility is trap-modulated. If this were the case, the mobility, μ_o, which is defined as the average distance travelled per unit field in the direction of the field in the time between collisions divided by the time-interval between collisions may be calculated from the equation:[5]

$$\mu_o = \mu N_t \sigma_t v_{th} / \nu e^{-E_t/kT} \qquad (8)$$

μ_o turns out to be 4.5 cm^2 V^{-1} sec^{-1}; thus the range per unit field, $\omega_o = \mu_o \tau_o$, is approximately 1.8×10^{-7} cm^2 V^{-1}. This value of ω_o suggests a situation wherein the charge carrier is trapped after traversing a distance of the order of the dimensions of a unit cell in the crystal. The value of σ_t is much too small to be associated with atomic or molecular dimensions. It is interesting to note that trapping cross-section of the order of 4×10^{-17} cm^2 was also reported for p-terphenyl by Mark and Helfrich.[6] It may be that the trapping mechanism is of the

---

[4] R. H. Bube, "Photoconductivity of Solids," John Wiley and Sons, Inc., New York (1960), p. 51.

[5] A. Rose, R. C. A. Rev., 12, 362 (1951).

[6] P. Mark and W. Helfrich, op. cit., vol. 33, p. 205.

type suggested by Landau, that of an electron digging its own potential hole.[7] A positive hole could be trapped similarly. It is conceivable that such a trapping mechanism in organic molecular solids may give a suitable explanation for the small value of σ_t. Using the value for ω_o, the saturation voltage, $V_s = d^2\omega_o$, is found to be approximately 140 volts. The value of the saturation voltage is well within the sublinear region of the J_d vs. V curve and supports very strongly the statement made previously regarding the nature of the sublinear portion of curve 1.

Curves 2,3,4,5,6,7, and 8 are the current-voltage characteristics at various intensities and/or modes of illumination. Curve 2 was taken while the conductivity cell was excited by 240 mμ monochromatic light. Light of this wavelength is almost completely absorbed by the SnO_2 film and only a very small fraction of the incident light intensity reaches the crystal. The relatively weak optical excitation did not affect significantly the uniformity of the distribution of the free charge carriers in the crystal as is evidenced by the ohmic characteristic of the curve at the low voltage range. The effect of seriously disturbing the uniformity of the charge carrier distribution in the crystal is shown by curves 3 and 4 which were taken using light with wavelengths of 320 and 370 mμ respectively. Light of these wavelengths is transmitted almost completely through the SnO_2 film and is strongly absorbed by the crystal within a surface layer of a few hundred Angstrom thickness. These photons are quite efficient for photoproduction of charge carriers. It is seen that both curves are strictly superlinear, the current increasing as $V^{1.6}$. Curves 5,6, and 7 were obtained using polychromatic light at different intensity levels by interposing between the light source and the cell, neutral optical density screens rated at 1.5, 1.0 and 0.5 optical density units respectively. Curve 8 was obtained at 100% light intensity. By using polychromatic light, it

---

[7] L. Landau, Physik. Z. Sowjetunion, 3, 664 (1933).

was hoped that a smoothing out of the charge carrier distribution could be effected even when the crystal is operated under a higher rate of photo-excitation. Since light of wavelengths which are more effective for carrier generation are usually mostly absorbed close to the illuminated surface, a strictly uniform distribution of charge carriers throughout the crystal can not be achieved. However, by adjusting the polychromatic light intensity it may be possible to bring about a balancing effect between the rate of charge carrier generation by the strongly absorbed component of the incident light at the surface layer and the generation of charge carriers in the bulk of the crystal by the weakly absorbed and other long wavelength components of the incident radiation. These expectations appear to have been realized. Thus in curves 5 and 6 which were obtained at lower light intensities, the current increased linearly with the voltage in the same range of voltages where linearity was previously observed in curve 2. Curves 7 and 8 which were obtained at higher light intensities show tendency to deviate from linearity. The deviation occurs at lower voltages and indicates that the charge carrier density at the surface layer may have become considerably greater than the density of charge carriers in the bulk of the crystal. Based on the current-voltage characteristics in the low voltage range as shown by curves 2 - 8 and especially by 3 and 4, it is concluded that the superlinearity of the current-voltage characteristics may be caused solely by the non-uniformity of optical excitation of the crystal even in the range of voltages in which the unilluminated crystal may be expected to operate under uniform electric field conditions. In curves 2,5, and 6, the photocurrent is linear with applied voltage in approximately the range of voltages where the saturation of the dark current was previously observed (curve 1). On the basis of the Hecht equation this implies that the range, $\omega = E\mu\tau$, of the charge carriers had decreased as a result of photo-excitation, a consequence which might have been occasioned by decrease of either mobility, lifetime, or both. It seems reasonable to attribute this decrease of ω to a decrease of τ only, which may arise as the result of the increasing importance of charge

carrier recombination as a process limiting the density of free charge carriers when the crystal is illuminated. Unlike the dark current which increases as V^2 in the higher voltage range, the photocurrent in curves 2,5,6,7, and 8 increased as $V^{3/2}$. The $V^{3/2}$-dependence is interesting in that it is the current-voltage characteristics of this particular cell under conditions of illumination which were more or less uniform throughout the whole crystal. It must be emphasized, before going any further in this discussion, that the current-voltage characteristics of different sandwich cells of one compound are by no means predictable and that $V^{3/2}$-dependence at high electric field ranges is not with any great generality, a characteristic of m-terphenyl sandwich cells. In this particular case the result is rather unique in that the $V^{3/2}$-dependence occurs above the ohmic voltage range and makes it reasonable to assume that this effect is due either to the non-linear dependence on the electric field of the drift velocity of the charge carriers or to a voltage dependence of the kinetics of carrier generation.

The variation of the current as $V^{3/2}$ is characteristic of vacuum diodes and the relation between the current and the voltage is defined by the Child[8] - Langmuir[9] law

$$J = BV^{3/2} \qquad (9)$$

where B is a constant. Implicit in the derivation of this equation is that the kinetic energy, $1/2\ mv^2$, of the charge carrier is equal to the energy, eV, that the charge carrier gains from the electric field. Thus the velocity, $v = (2eV/m)^{1/2}$ and since the space charge, $Q = CV$, the current, $J \propto V^{3/2}$. In view of the fact that in a solid the charge carriers will have to move through a medium of high friction, a satisfactory explanation for the $V^{3/2}$-dependence of the photocurrent must

---

[8] C. D. Child, Phys. Rev., 32, 492 (1911).

[9] I. Langmuir, ibid., 2, 450 (1913).

retain the concept of a drift mobility which is independent of the electric field. On the basis of a model where the electrons are scattered by acoustical phonons, Shockley showed that at moderately high electric fields, i. e. electric fields not high enough to make scattering by optical phonons important, the drift velocity of the electrons varied as the square root of the electric field. The equation for the drift velocity is

$$v_d \simeq \upsilon \mu_o E^{1/2} \tag{10}$$

where υ is the velocity of the acoustical waves in the medium and μ_o is the lattice drift mobility of the charge carriers.[10] When it is considered that the electric field in the $V^{3/2}$ region in Fig. 1 ranges from 3×10^4 to 10^5 V/cm and that $\mu_o = 4.5$ cm^2/V sec, the microscopic drift velocities would be of the order of 10^5 cm/sec. This is of the same order of magnitude as the velocity of sound ($\sim 10^5$ cm/sec). According to Shockley's model, charge carriers with velocities approaching that of the acoustical waves would tend to become "hot" i. e. they would tend to gain energy from the electric field faster than they can lose this energy by collision with the acoustical phonons. It is even possible that the drift velocity of the charge carriers may exceed 10^5 cm/sec in an illuminated crystal because of the possibility of the formation of a well defined space-charge region a few microns thick at the illuminated side of the crystal and across which most of the applied voltage drops.[11] It seems, therefore, not too unreasonable to conclude that the $V^{3/2}$-dependence noted is due to "hot electrons" injected into the crystal. Thus analogous to the Child-Langmuir law, the $V^{3/2}$-dependence may be expressed as:

$$J = \Phi(\upsilon \mu_o C/d^{3/2})\ V^{3/2} \tag{11}$$

---

[10] W. Shockley, Bell Syst. Tech. J., 30, 990 (1951).

[11] A. von Hippel, E. P. Gross, J. G. Jelatis and M. Geller, Phys. Rev., 91, 568 (1953).

where ϕ is the fraction of hot electrons in the injected space-charge and the rest of the symbols are as previously defined. ϕ is left without an analytic definition and will serve for the present as an adjustable parameter.

On the other hand, the $V^{3/2}$-dependence may represent some upper limit of a voltage-dependent kinetic process. It was previously mentioned that the shortening of the lifetime of the charge carriers is the probable cause of the linearity of the photocurrent with voltage in the range of voltages where the dark current was found to be sublinear. The most elementary process that might be invoked is a "bimolecular" type of recombination, the effective recombination rate "constant", R_{eff}, being a function of the electric field:

$$[\ \partial n(V)/\partial t\ ]_{V,I} = L - R_{eff} n^2 \qquad (12)$$

where L is the rate of photogeneration, $n = n_+ = n_-$ is the density of the free holes or electrons in the illuminated layer of thickness b. Under steady state condition

$$n = (L/R_{eff})^{1/2} \qquad (13)$$

We assume a convenient form of R_{eff} such as:

$$R_{eff} = R_b(1-e^{-b/E\mu_o\tau_b}) \qquad (14)$$

where R_b is the characteristic bimolecular rate of recombination in the illuminated layer and τ_b is the "life time" of the charge carriers in this layer.

$$n = [\ L/R_b(1-e^{-b/E\mu_o\tau_b})\ ]^{1/2} \qquad (15)$$

For electric fields such that $5E\mu_o\tau_b \leq b$

$$n = (L/R_b)^{1/2} \qquad (16)$$

and for high electric fields such that $E\mu_o\tau_b \geq 25b$

$$n = [\ L/R_b(b/E\mu_o\tau_b)\ ]^{1/2} \qquad (17)$$

Since the current, $J = ne\mu_o E/d$ it is seen that at low voltages, $J \alpha V$ and at higher voltages $J \alpha V^{3/2}$. Since the transition from an electric field-independent to an electric field-dependent rate of recombination depends upon b, it is seen that when b is small as in the case when the exciting light is strongly absorbed close to the crystal surface, the transition from the ohmic to the super-linear current-voltage characteristics will occur at lower voltages. This provides a qualitative explanation for the general tendency of curves 2,5,6,7, and 8 to become super-linear at lower voltages and the observation of a strictly super-linear characteristic of 3 and 4. To get an approximate value of τ_b we assume that the electric field, $E \sim 10^4$ V. cm^{-1} at the transition from a V- to a $V^{3/2}$-dependence, satisfies the condition $5 E\mu_o\tau_b = b$ and that $b = 10^{-5}$ cm. τ_b turns out to be of the order of 10^{-9} sec. On making the assumption that the recombination cross-section, $\sigma_{rb} = 10^{-15}$ cm^2, the density of recombination centers, N_{rb}, in the illuminated region turns out to be of the order of 10^{19} cm^{-3}. These estimated values are rather interesting in that they imply the molecular nature of the recombination centers.

It is not possible presently to discriminate between the two alternative interpretations of the super-linear character of the current-voltage curves. Further work is necessary to ascertain the nature of the scattering mechanisms for charge carriers and the nature of the recombination centers in organic molecular solids.

p-Quarterphenyl, p-Terphenyl and Anthracene: The current-voltage characteristics of a 35 micron-thick crystal of p-quarterphenyl are shown in Fig. 3. In curve 1 the dark current, J_d, is slightly super-linear. The slope of log J_d vs. log V. in the range of voltages from 10 to 120 volts is 1.2. There is a tendency for the dark current to increase as V^2 at higher voltages. Curve 2 shows the current-voltage relationship when the crystal was illuminated with polychromatic light through the positive electrode. The photocurrent, J_{p+}, increased as $V^{1.6}$ between 2 and 70 volts while in curve 3, the photocurrent when the illuminated side was negative J_{p-}, increased as $V^{1.5}$ within the same range of

Fig. 3. Current-Voltage Characteristics: p-Quarterphenyl

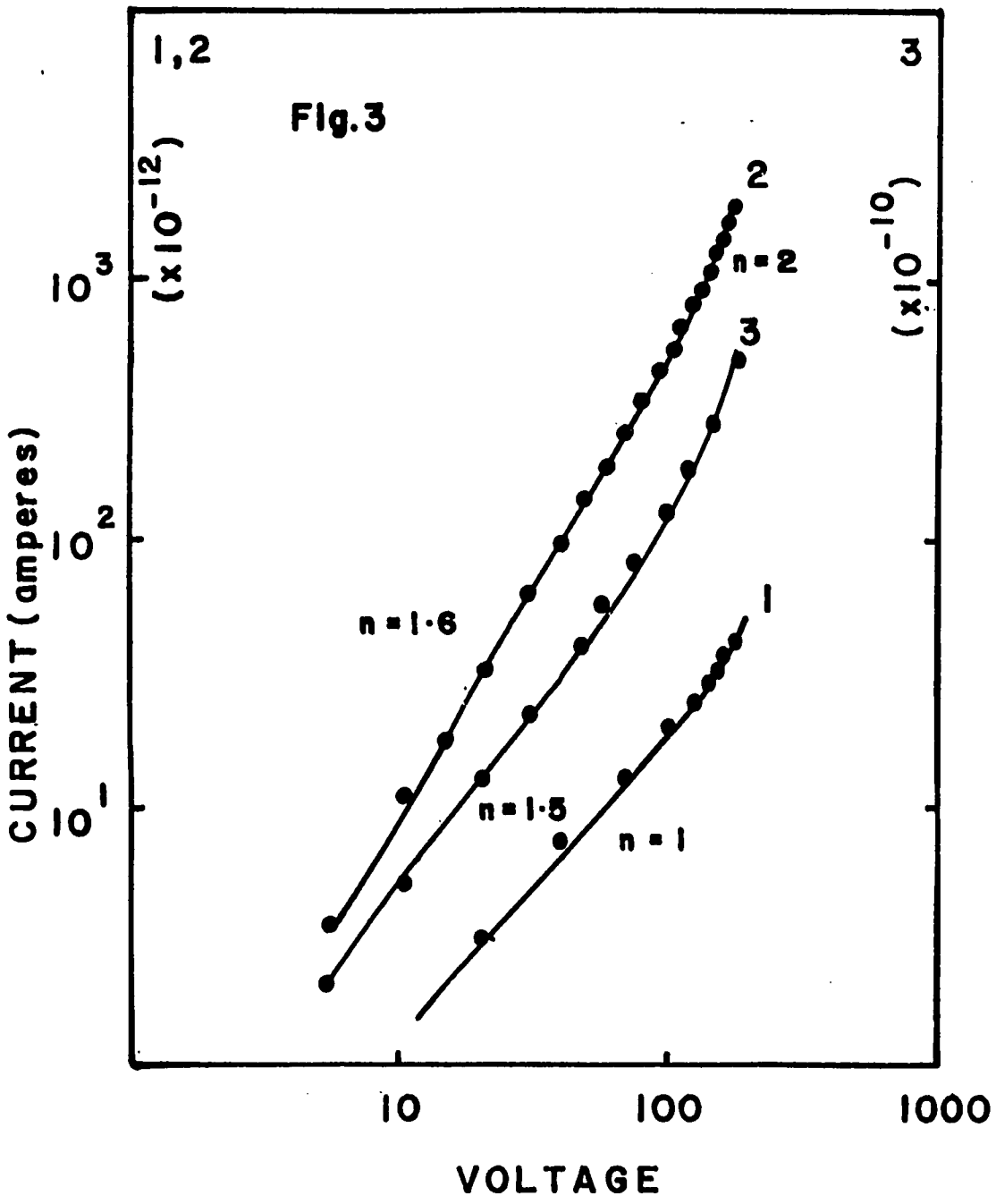
1,2
3
Fig.3
(x10^-12)
(x10^-10)
2
n=2
3
n=1·6
1
n=1·5
n=1
10^3
10^2
10^1
CURRENT (amperes)
10
100
1000
VOLTAGE

voltages. Both currents increased as V^2 at voltages greater than 100 volts. The transition of the dependence of J_{p+} and J_{p-} from a $V^{1.6}$ and $V^{1.5}$ respectively to a V^2-dependence is not quite sharp. However, in the J_{p+} curve transition from the $V^{1.6}$ to the V^2-dependence appears to be at V = 100 volts. Similarly in curve 3, this occurs at approximately V = 90 volts. These voltages, which will be referred to as the transition voltages, probably represent, respectively, the critical voltages for the extraction of electrons from the illuminated crystal surface in the case of J_{p+}, and the injection of electrons into the illuminated crystal surface in the case of J_{p-}. Thus in the case of J_{p+} a positive space charge due to trapped holes is formed in the crystal and in the case of J_{p-}, a negative space charge resides in the bulk of the crystal due to trapped electrons. The lack of any spectacular increase of the current with voltage below the V^2 region and the relatively low space-charge-limited (SCL) current densities indicate the presence of relatively high densities of discrete trapping centers for both the holes and the electrons in the crystal. The higher SCL current density obtained for J_{p+} compared to that for J_{p-} implies that the density of trapping centers for holes is less than that for the electrons and/or the mobility of the holes is greater than that of the electrons. If the trapping states were distributed more or less exponentially in energy, the current below the V^2 region would have increased according to the well known equation for a space charge-limited-trap-filled-limited (SCL-TFL) current:

$$J = 10^{-13}(V\mu_o\varepsilon/d^2)(en_{co}/C)\ e^{\gamma V} \qquad (18)$$

Where n_{co} is the initial thermal equilibrium concentration of the free carriers, where $\gamma = C/(n_t dekT)$, where n_t is the number of traps per cubic centimeter per unit range of energy, and where C is the capacitance of the crystal.[12] A current which obeyed the above

---

[12]Rose, op. cit., vol. 97, p. 1538.

relationship was obtained in p-terphenyl and is depicted in Fig. 4. There is, however, an anomaly below 40 volts. According to Eq. (18) the transition in the low voltage range should be from an ohmic to a SCL-TFL current. The current-voltage curve below 40 volts is superlinear; the current increasing as $V^{3/2}$. This anomaly may be due to the effects of voltage which were previously discussed. However, between 40 and 150 volts, there is no question regarding the characteristics of the current. It increased as V^5 and above the transition voltage, V = 150 volts, it increased as V^2. The change from the V^5-dependence to the V^2-dependence indicated that at 150 volts the trapping centers were completely filled. SCL-TFL currents were also obtained by Mark and Helfrich[13] using electrolyte electrodes. In their work, the transition from SCL-TFL to SCL characteristics were not obtained because the current saturated before the transition voltage was reached.

Current-voltage characteristics which appear to behave as SCL-TFL currents were found in a 40 micron-thick crystal of anthracene and are shown in Fig. 5. In curve 1, $J_d \propto V^{2.2}$ between 10 and 76 volts and $J_d \propto V^9$ above 76 volts. In curve 2, J_{p+} increases as $V^{1.3}$ between 5 and 50 volts, and as V^4 at higher voltages. In curve 3 J_{p-} is sublinear, increasing only as $V^{0.6}$ between 5 and 50 volts and exhibiting a "break-away" characteristic above 50 volts. The positive identification of the rapidly rising portions of curves 1 and 2 was not unambiguously proved to be or not to be due to SCL-TFL current. There is reason to believe that the rapid increase in the current with voltage is due to the onset of dielectric breakdown. Attempts to observe a saturation of the current with voltage or a transition toward a V^2 dependence at higher voltages were not successful because the cells usually breakdown permanently and were consequently short-circuited. The occur-

---

[13] Mark and Helfrich, op. cit., vol. 33, p. 205.

Fig. 4. Current-Voltage Characteristics: p-Terphenyl

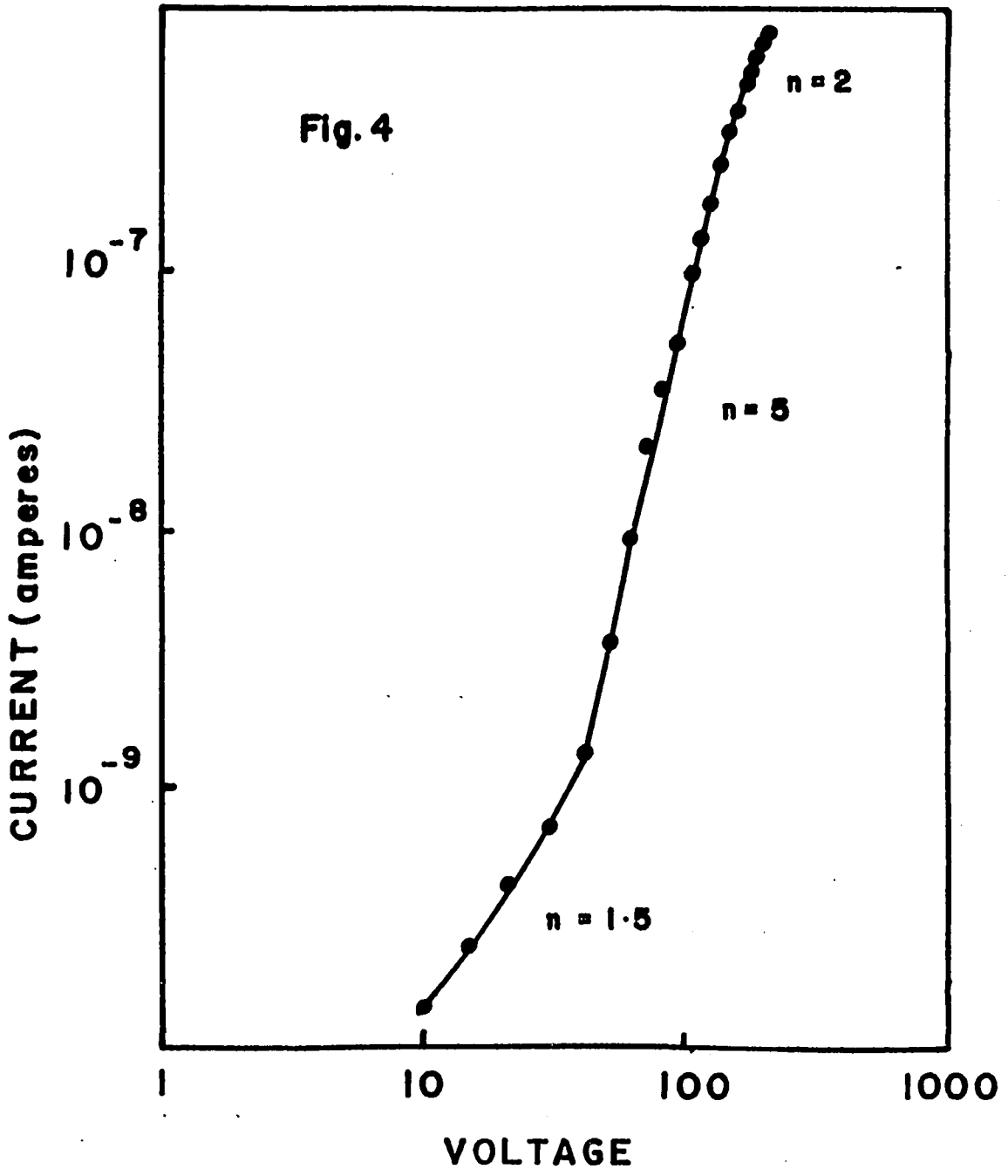
Fig. 4
n = 2
n = 5
n = 1·5
10^{-7}
10^{-8}
10^{-9}
CURRENT (amperes)
1
10
100
1000
VOLTAGE

Fig. 5. Current-Voltage Characteristics: Anthracene

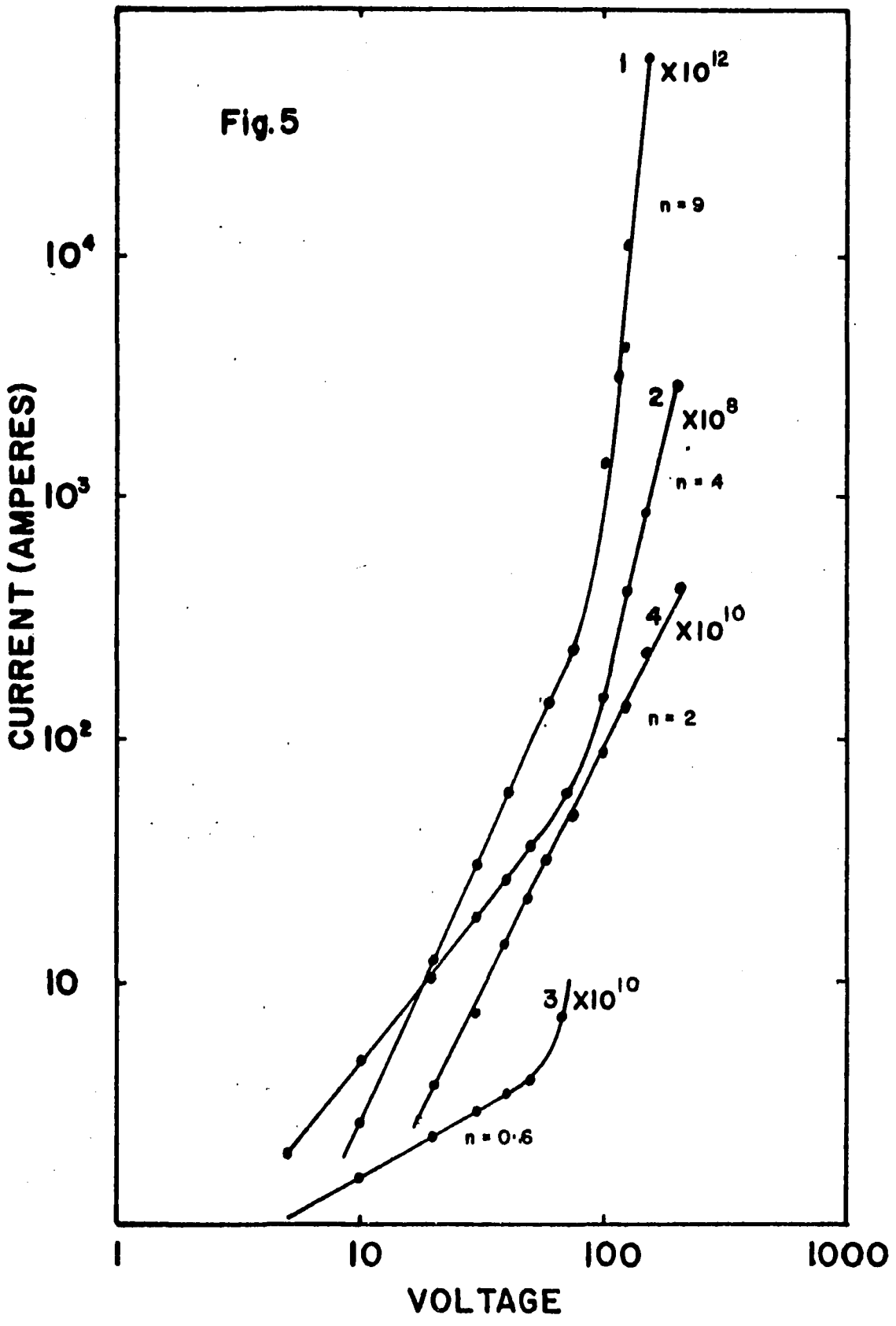
Fig. 5
1 X10^12
n = 9
2 X10^8
n = 4
4 X10^10
n = 2
3 X10^10
n = 0·6
CURRENT (AMPERES)
10^4
10^3
10^2
10
1
10
100
1000
VOLTAGE

rence of dielectric breakdown lends credibility to the belief that the sharp rise of the current with voltage is due to the onset of this phenomenon. Several mechanisms have been proposed by several authors to explain the phenomenon of dielectric breakdown but none of these may be ruled out with any great degree of certainty on the basis of the results presented in Fig. 5. There is, however, the experimental result shown by curve 4 which enables us to eliminate several possibilities. Curve 4 was obtained when the crystal was cooled down to approximately 150°K. The cell was illuminated through the positive electrode with polychromatic light. It is seen that $J_{p+} \alpha V^2$ throughout the voltage range. Since no unusual rise in the current was observed in 4, it may be concluded that neither the breakdown mechanism due to electron multiplication as suggested by Von Hippel[14] nor the Zener[15] type of dielectric breakdown were the operative processes. It is, however, possible that the breakdown is due to joule heat as suggested by Wagner[16]. If this were the case the sharp rising portions of curves 1 and 2 may have been due to the thermal ionization of impurity centers and the detrapping of charge carriers caused by local heating and not due to an SCL-TFL current. From the available experimental data, the trapping state density for holes in anthracene may be calculated. The conductivity glow curve shown in Fig. 6 yielded a trap depth, E_t = 0.6 ev, for the main glow peak. Using the values: μ_o = 2 cm^2/V sec, $N_c = 2.5 \times 10^{19}$ cm^{-3}, ϵ = 2.5, $d = 4 \times 10^{-3}$ cm, T = 150°K and the current density at V = 100 volts from curve 4 which is, $J_{p+} = 8.8 \times 10^{-9}$ amps./1.5 cm^2, N_t turns out to be 10^{18} cm^{-3}.

---

[14] A. von Hippel, Z. Physik, 75, 145 (1932).

[15] C. Zener, Proc. Roy. Soc., 160A, 523 (1934).

[16] K. W. Wagner, Elec. Eng., 41, 1034 (1922).

Fig. 6. Conductivity Glow-Curve: Anthracene

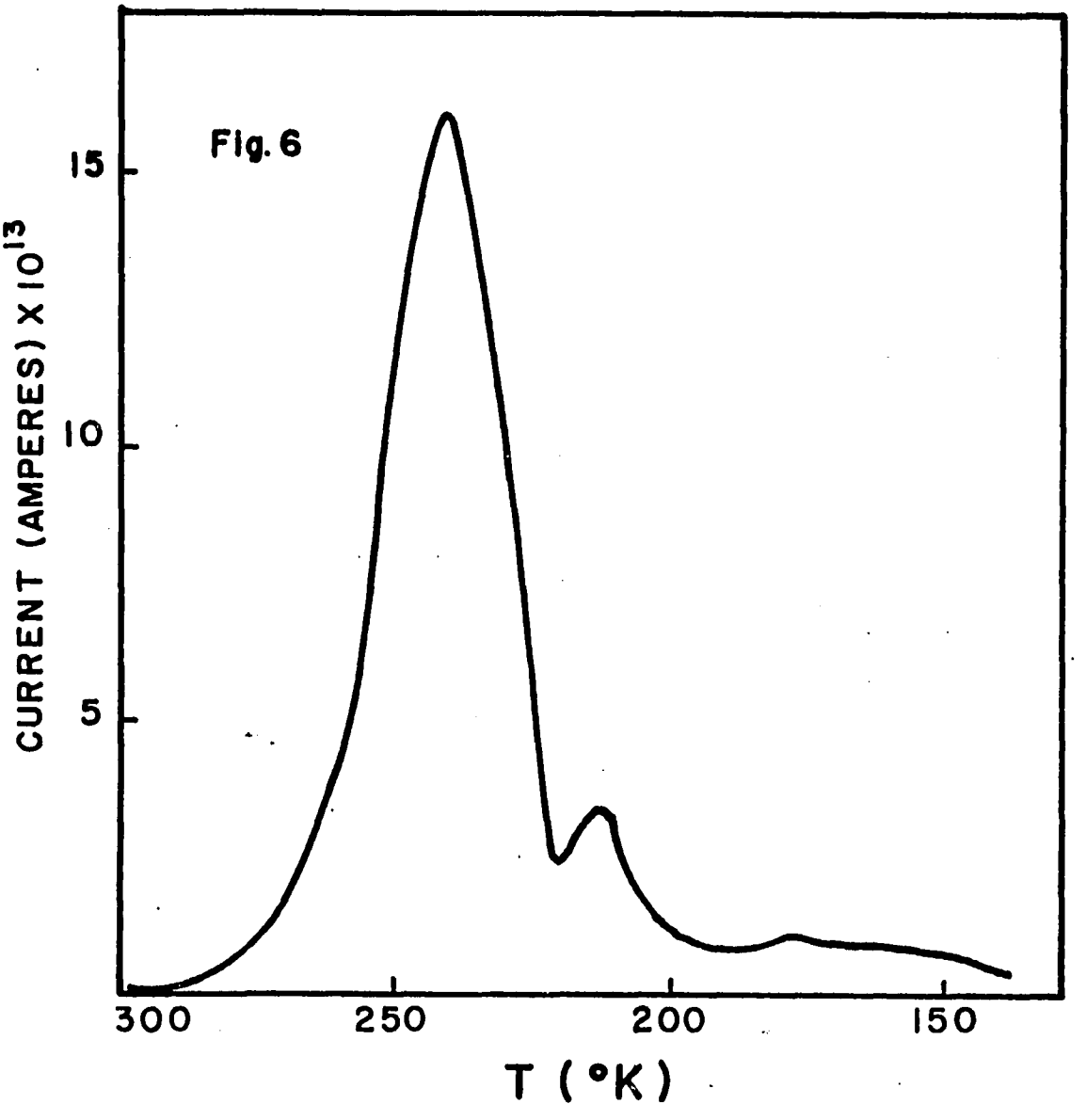
Fig. 6
CURRENT (AMPERES) X 10^13
15
10
5
300
250
200
150
T (°K)

The current-voltage curves 2 and 3 are quite similar to the forward and the reverse current-voltage characteristics of pn junctions.[17] Rectifying junctions arising from the presence of surface states as proposed by Bardeen[18] and Bardeen and Brattain[19] and from the mismatch of the work function of electrode and the crystal as suggested by Mott[20] and Schottky[21] are also probable causes of the superlinear character of the current-voltage characteristics in Fig. 5.

Biphenyl and Tetraphenylbutadiene: The current-voltage characteristics of a 30 micron-thick crystal of biphenyl are shown in Fig. 7. The dark current (see curve 1) increases as V^2 below 7 volts. At voltages between 7 and 50 volts it increases linearly with voltage. The current becomes extremely noisy at higher voltages. The behavior of the photocurrent with voltage when the cell was illuminated with polychromatic light through the positive electrode is shown by curve 2. The current varies as $V^{1/2}$ below 50 volts and between 50 and 180 volts the photocurrent becomes extremely noisy. The onset of noise is usually followed by dielectric breakdown. The breakdown cuases the cells to be short circuited.

The V^2-dependence of J_d at low voltages and the change of this dependence to ohmic characteristic at higher electric fields may be analyzed in terms of the equation derived by Mott and Gurney[22] for the dependence of current on voltage for smaller electric fields for which the space-charge is important. The equation they derived for the

---

[17] W. Shockley, Proc. I. R. E., 40, 1289 (1952).

[18] J. Bardeen, Phys. Rev., 71, 717 (1947).

[19] J. Bardeen and W. H. Brattain, ibid., 75, 1208 (1949).

[20] N. F. Mott, Proc. Roy. Soc., 171A, 27 (1939).

[21] W. Schottky, Z. Physik, 118, 539 (1942).

[22] N. F. Mott and R. W. Gurney, "Electronic Processes in Ionic Crystals," Clarendon Press, Oxford (1948), p. 172.

Fig. 7. Current-Voltage Characteristics of Biphenyl

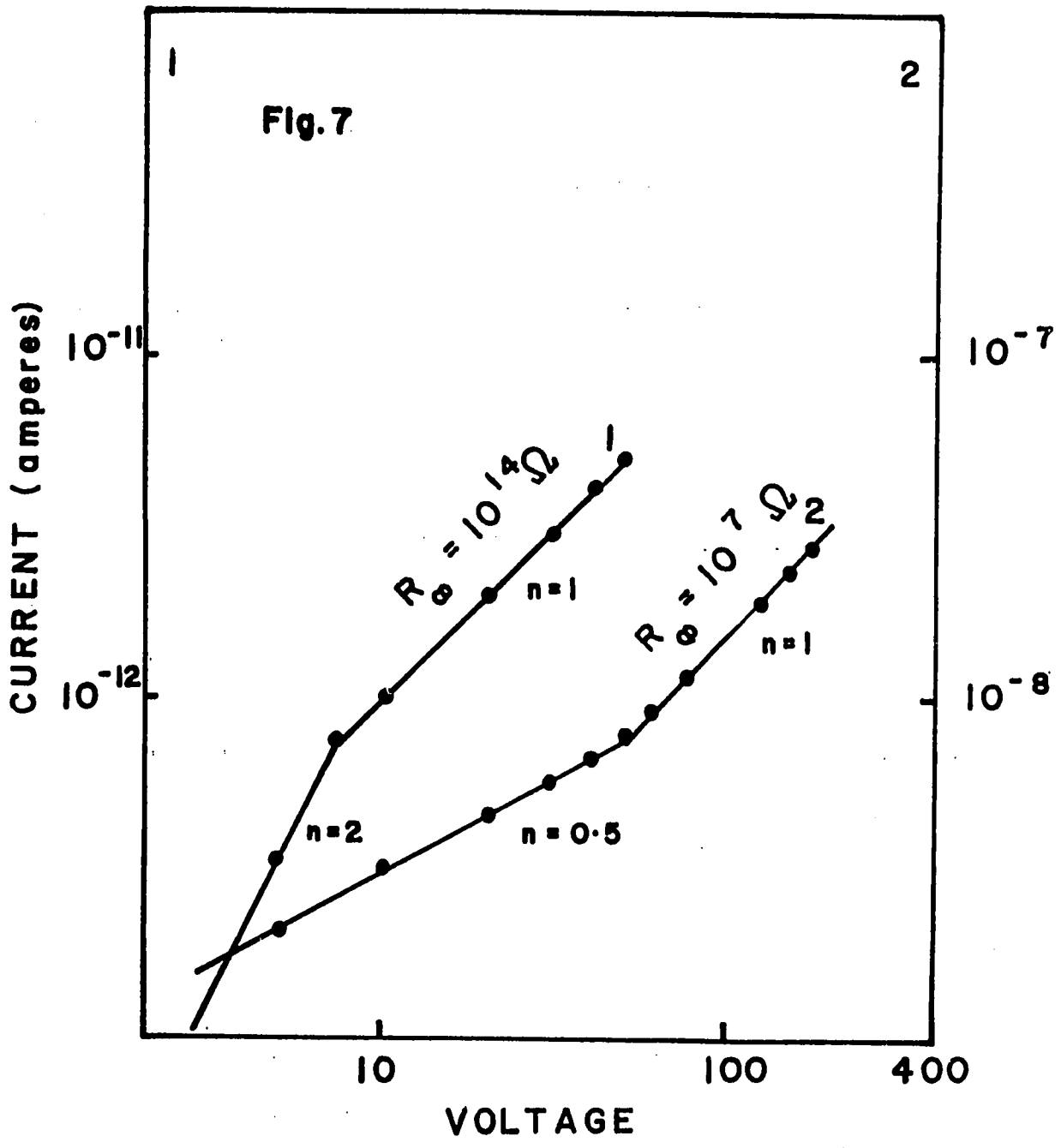
1
2
Fig. 7
CURRENT (amperes)
10^{-11}
10^{-12}
10^{-7}
10^{-8}
$R_\Theta = 10^{14}\Omega$ 1
$R_\Theta = 10^{7}\Omega$ 2
n=1
n=1
n=2
n=0.5
10
100
400
VOLTAGE

potential drop across the crystal is:

$$V = 2/3\ (8\pi J/\mu)^{1/2}\ [(d + b_o)^{3/2} - b_o^{3/2}] \qquad (19)$$

$$b_o = J/8\pi\mu N_o^2 e^2 \qquad (20)$$

N_o is the density of the electrons at the surface immediately in contact with the electrode, b_o is a constant and the rest of the symbols are as defined previously. The two equations give J in terms of V. For small values of V, J is small and $b_o \ll d$ so that

$$J = 9\mu V^2/32\pi d^3 \qquad (21)$$

The current increases as V^2. For large voltages $b_o \gg d$ whence

$$J = e\mu N_o V/d \qquad (22)$$

The current is ohmic. The order of magnitude of the critical field is therefore:

$$E_c = V/d \gtrsim eN_o d \qquad (23)$$

The last equation allows the calculation of the order of magnitude of N_o from the transition voltage, V = 7.2 volts, in curve 1. It turns out that $N_o \lesssim 5.5 \times 10^{12}$ cm^{-2}. We note that the dark currents in Fig. 7 are of the order of 10^{-13} amperes in the space charge region of the J_d curve. If all of the N_o charge carriers were free, the value of μ calculated from Eq. (22) would be of the order of 10^{-10} cm^2 V^{-1} sec^{-1} which is a very unreasonable number! On the other hand, if we assume a reasonable value for the mobility, $\mu \sim 1$ cm^2 V^{-1} sec^{-1}, the current calculated from the same equation would be of the order of a milli-ampere. It must, therefore, be concluded that these charge carriers are mostly immobilized. It is quite possible that they are localized in the surface states of the crystal particularly in the immediate vicinity of the crystal-electrode contact. If this were the case we could obtain an estimate of the density of surface states from the estimated density of surface charge when the crystal is operated under a condition in which it may be

reasonably assumed that the surface states are almost completely occupied, i. e. the rate of charge carrier generation in the crystal must be made sufficiently high to maintain the highest possible density of free charge carriers. In curve 2, which we shall discuss later, we note that the transition voltage, V = 50 volts has increased by nearly an order of magnitude compared to that of curve 1. The value for N_o is 5×10^{13} cm^2. This value, if taken as an estimate of the surface state density, seems to be very reasonable when compared to the estimated and measured densities of surface states in some inorganic crystals. There is presently no available data for the density of surface states in organic crystals. In a hypothetically clean and perfect germanium or silicon surface, the surface state density was estimated by Shockley[23] to be of the order of 10^{14} to 10^{15} cm^{-2} while the experimentally measured surface state density in n-type germanium is of the order of 5×10^{13} cm^{-2} according to Shockley and Pearson.[24]

The filling up of the surface states gives rise to a space-charge layer near the surface; a potential barrier is established at a value such that the excess charge in the surface states is balanced by that of the ionized impurities and the free carriers in the space-charge layer. The potential barrier may be estimated from the dark current curve. At the transition voltage, the free charge carrier density, n_f, in the bulk must equal that at the surface. From the ohmic region of the curve we calculate the ohmic resistance, $R = d/n_v e\mu = 10^{14}$ ohm/cm^{-2} and assuming that $\mu \sim 1 cm^2 V^{-1} sec^{-1}$ we get $n_f = 150$ charge carriers per cm^3. Using the equation $n_f = N_o e^{-V_b/kT}$ with kT = 1/40 ev., V_b is found to be 0.7 to 0.8 ev.

The externally applied voltage changes the potential drop across the barrier and hence results in a change in the thickness of the barrier.

---

[23] W. Shockley, Phys. Rev., 56, 317 (1939).

[24] W. Shockley and G. L. Pearson, ibid., 74, 232 (1948).

If the sense of the applied voltage is in the forward direction i. e. the barrier height is decreased, the width of the barrier, b_o, increases as deduced from the barrier equation:[25]

$$V_b \mp V = (2\pi/\epsilon)\ n_d e b_o^2 \qquad (24)$$

Conversely when the applied voltage is in the reverse direction, b_o decreases. The $V^{1/2}$-dependence of J_{p+} may be due to the photogeneration and recombination taking place mainly in the space charge region: J_{p+} being in this sense taken as the reverse current.[26]

The photocurrent-voltage characteristics of a 28 micron-thick crystal of tetraphenylbutadiene are shown in Fig. 8. The crystal was excited with monochromatic light at 365 mμ. The characteristics are very similar to those obtained for biphenyl except that in tetraphenylbutadiene, the J_{p+} curve varies as V^2 in the range of low voltages. In biphenyl J_{p+} is proportional to $V^{1/2}$. This difference probably arises from the difference in the polarity of the surface charge in the two compounds. This suggests the possibility that the majority carriers in biphenyl have the opposite sign to that in tetraphenylbutadiene.

---

[25] A. J. Dekker, "Solid State Physics," Prentice-Hall, Inc., Englewood Cliffs, N. J., (1961) p. 350.

[26] W. Shockley and W. T. Read, Phys. Rev., 87, 835 (1952).

Fig. 8. Current-Voltage Characteristics: Tetraphenylbutadiene

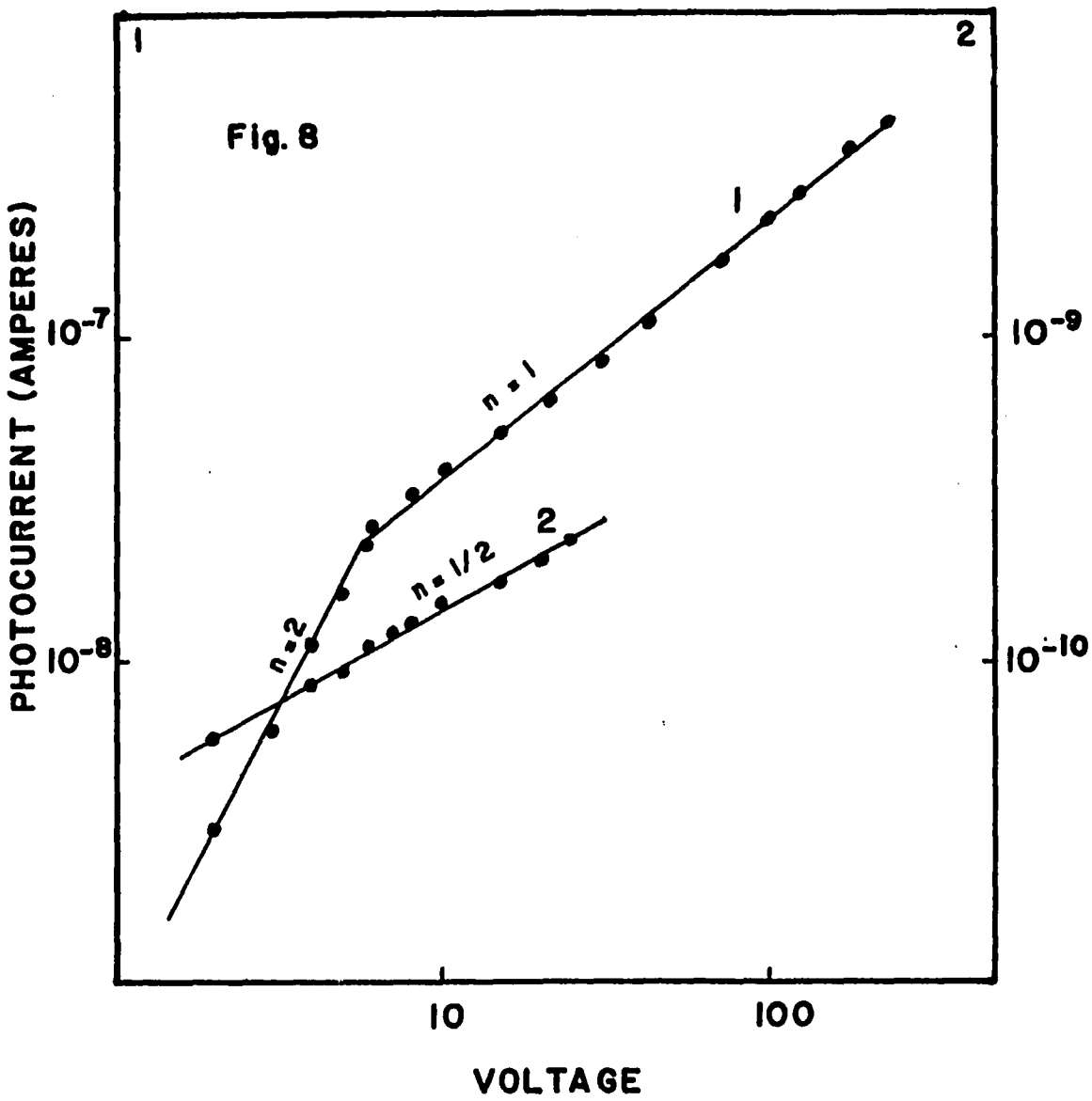
Fig. 8
1
2
PHOTOCURRENT (AMPERES)
10^{-7}
10^{-8}
10^{-9}
10^{-10}
n = 1
n = 1/2
n = 2
1
2
10
100
VOLTAGE

B. Dependence of Photocurrent on Light Intensity

The results obtained from the study of the variation of the photocurrent with light intensity may be expressed in terms of the relationship, $J_{p+} \propto I_{\lambda}^{m}$, where J_{p+} is the photocurrent when the illuminated side is positive, I is the intensity of the incident light of wavelength λ, and $0.5 \leq m \leq 1$. Where polychromatic light is used, the photocurrent is linear with light intensity. Log J_{p+} was plotted against log $\%I_{\lambda}$ for different compounds. The values of m were calculated. The results are summarized in Table I. It is observed that:

(a) The photocurrent is linear with light intensity when the light is almost completely absorbed at or very close to the surface of the crystal. The penetration depth of the short-wavelength light used is probably less than 10^{-5} cm.

(b) The photocurrent is approximately proportional to the square root of the light intensity when the exciting light penetrates deeper into the bulk of the crystal. Based on 99% absorption, the extinction coefficient and the density of the crystal, the penetration depth of the light of longer wavelength used for excitation was estimated to be of the order of 1 micron.

(c) The exponent, m, tends to increase with increase of the voltage applied across the crystal.

These observations as well as others concerning the effect on the photocurrent-voltage characteristic of various modes of illumination may be rationalized with a fair degree of consistency. From the super-linear J_{p+} vs. V characteristic that invariably results when the crystal is excited by a strongly absorbed monochromatic light, it may be assumed that a potential barrier is established when the crystal is illuminated. This potential barrier might be of the Schottky type or of the type that might arise because of the presence of surface states in the crystal. For the purposes of the discussion, let it be assumed that the barrier is formed because the surface of the crystal in contact with the SnO_2 electrode is charged negatively, and that adjacent to the surface and extending into the bulk of the crystal there is a positive

TABLE I

Intensity Dependence of Photocurrent

Compound	Volts	λ(mμ)	m
biphenyl	12	270	1.00
m-terphenyl	30	310	0.66
	30	370	0.61
	150	310	0.87
	150	370	0.75
tetraphenylbutadiene	23	365	0.98
	23	435	0.48
	80	365	1.03
	80	435	0.58
anthracene	12	390	1.00
	12	420	0.60

space-charge region of thickness, b. This space-charge region will be subsequently referred to as the depletion region or layer. There will, therefore, be a potential difference, V_b, between the surface and the bulk of the crystal such that an electron coming from below the surface has to acquire energy equal to eV_b in order that it can go over this potential barrier. Since the greater fraction of the voltage applied across the crystal drops across the barrier it seems quite possible that when a hole-electron pair is produced at the junction between the negatively charged surface layer and the depletion region, they may be immediately separated, before they can recombine, by the intense electric field at the junction. Thus the electron is extracted at the illuminated anode and the hole drifts through the bulk of the crystal wherein it may undergo trapping and detrapping before reaching the cathode. Clearly, the free hole density will be mainly limited by the extent of trapping in the bulk. This being a first order process, it follows that if $n_+ = n_- = \eta I_\lambda$, the current density J_{p+}, will be proportional to the incident light intensity when the light of wavelength λ is absorbed extremely close to the surface. On the other hand if the wavelength of the exciting light is such that the light is able to penetrate deeper into the crystal giving rise to pair production in the depletion region, the less energetic electrons will not be able to go over the barrier and will, therefore, have to remain in this region. As one consequence, the rate of recombination between the free charge carriers may dominate the limiting kinetics for the free charge carrier densities in the crystal. In this case, the square of the free electron-hole pair density will be proportional to the light intensity and therefore, J_{p+} will be proportional to the square root of light intensity. The observed increase of the exponent, m, of the light intensity with the increase in the voltage applied across the crystal may be reasonably attributed to the decrease of the free electron concentration in the depletion layer due to the lowering of the potential barrier by the applied voltage. The rate of recombination may then become less important compared to the rate of trapping.

Thus the dependence of J_{p+} on light intensity may be expected to change over from a square root to a linear dependence with increasing applied voltage.

C. Wavelength Dependence of Photocurrent

The Polyphenyls: The photoconduction action spectra of the polyphenyls are shown in Fig. 9. It is noted that in the series: biphenyl, m-terphenyl, p-terphenyl, p-quarterphenyl, the photoconduction peaks successively shift toward the red. With the exception of biphenyl, the photocurrent densities increase in the same order. The absorption of the incident light by the tin dioxide film makes it difficult to locate accurately the photoconduction peaks. The red shift, however, appears to be real. The "photoconduction threshold" (i. e., the wavelength of the exciting light at which a fairly abrupt rise in the photocurrent is observed on the long-wavelength side of the photoconduction peak) shifts in the same direction as the observed photoconduction peaks. The displacement of the photoconduction band toward the red in the series: biphenyl, p-terphenyl, p-quarterphenyl agrees with the generally expected direction of shift of the absorption bands in the same series. The red shift of the photoconduction band of m-terphenyl relative to that of the biphenyl is quite interesting since both of these compounds in solution show a single absorption band which peaks at 250 mμ. This observation suggests that the fundamental absorption band of m-terphenyl undergoes a greater red shift in going from solution to crystal than that of the biphenyl, which is not unexpected in view of the higher transition moment of the m-terphenyl species.

In so far as the series: m-terphenyl, p-terphenyl, p-quarterphenyl is concerned it may be concluded that the increasing extinction coefficient of the excitation to the first singlet excited state and the increase of intramolecular interaction enhance the photosensitivity of these materials. The large current density observed for the biphenyl is most probably due to some extrinsic factors, one of which would be the space charge characteristics of the J_p vs. V curves discussed previously.

Fig. 9. Photoconduction Action Spectra of the Polyphenyls

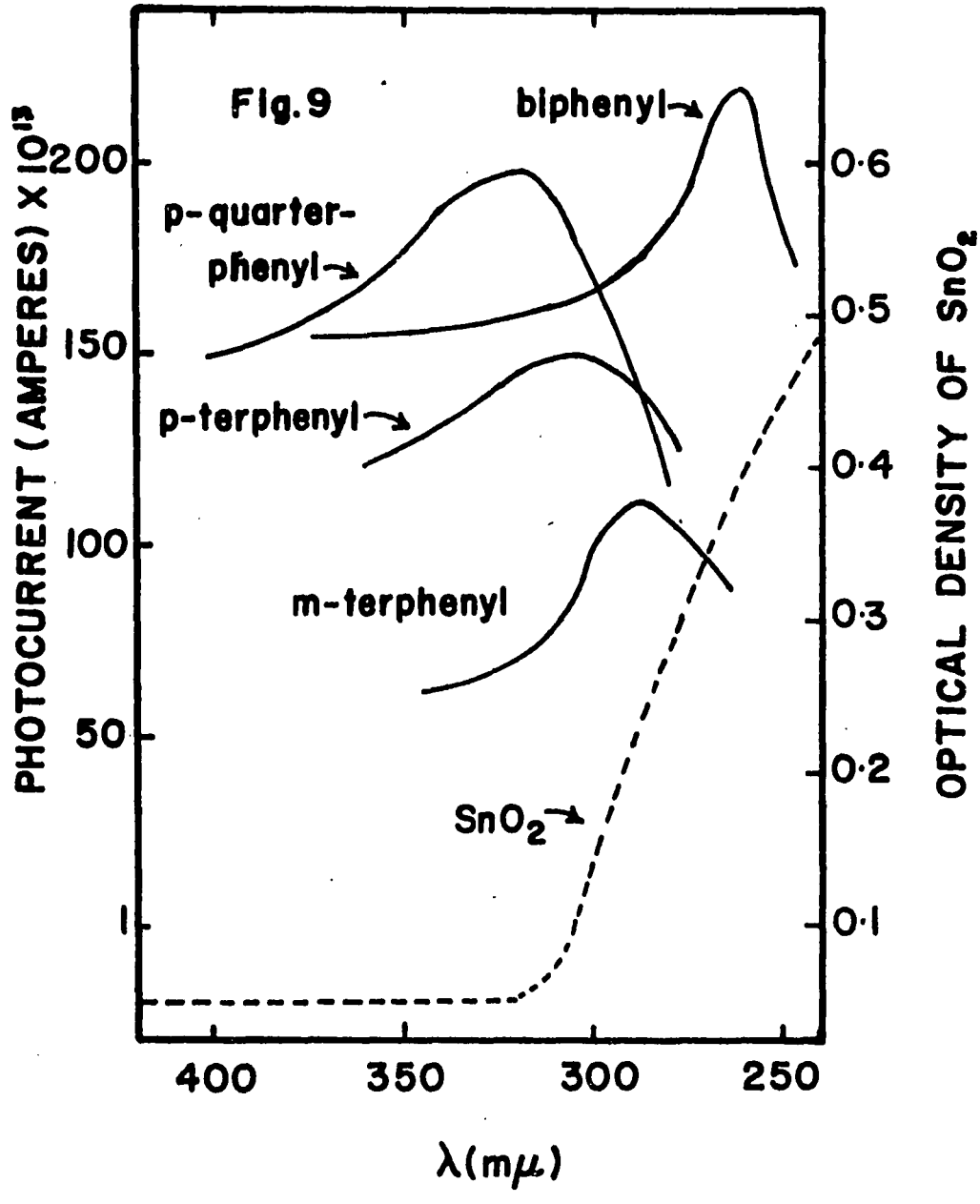
Fig. 9
biphenyl
p-quarter-
phenyl
p-terphenyl
m-terphenyl
SnO2
PHOTOCURRENT (AMPERES) X 10^13
200
150
100
50
1
0·6
0·5
0·4
0·3
0·2
0·1
OPTICAL DENSITY OF SnO2
400
350
300
250
λ(mμ)

Anthracene, Rubrene and Tetraphenylbutadiene: Fig. 10 shows the photoconduction action spectrum of anthracene and the b-polarized absorption spectrum of the crystal. The photocurrent spectral response curve remains practically flat between 480 and 445 mμ, and contains three main peaks; the most intense one is at 400 mμ, the least intense one is at 375 mμ and the one of intermediate intensity shows a splitting, peaking at 355 and 345 mμ. The relatively high photosensitive region spans the wavelength range 445 to 320 mμ, a band spread covering the whole wavelength range of the fundamental absorption band of the crystal. The peaks of the b-polarized absorption spectrum of the crystal reported by Craig and Hobbins[27] are at 393.1, 373.5, and 352.9 mμ. The main peaks in the photoconduction action spectrum are compared with the peaks of the crystal absorption spectrum in Table II. It is seen that the photoconduction maxima are shifted toward longer wavelength relative to the corresponding maxima in the absorption spectrum. A similar observation was reported for sandwich cells by Compton, Schneider and Waddington[28] and by Kommandeur.[29] The above authors, furthermore, reported that the maxima in the photoconduction action spectrum correspond to the minima of the crystal absorption spectrum and vice versa. The result shown in Fig. 10 is not entirely in accord with the last statement. In Fig. 10 the minima of the spectral response curve do not coincide with the maxima of the absorption curve. On the other hand, Kepler[30], using a similar electrode arrangement but with pulsed excitation, obtained a photoconduction action spectrum which reproduced the absorption spectrum of the crystal and a photocurrent which was linear with light intensity. Using "surface cells" (i. e., cells in which the

---

[27] D. P. Craig and P. C. Hobbins, J. Chem. Soc., 2309 (1955).

[28] D. M. J. Compton, W. G. Schneider and T. C. Waddington, J. Chem. Phys., 27, 160 (1957).

[29] J. Kommandeur, Ph. D. Dissertation, University of Amsterdam, February 19, 1958.

[30] R. G. Kepler, Phys. Rev., 119, 1226 (1960).

Fig. 10. (a) Photoconduction Action Spectrum of Anthracene
(b) b-Polarized Crystal Absorption Spectrum
(c) Absorption Edge of Anthracene Sandwich Cell

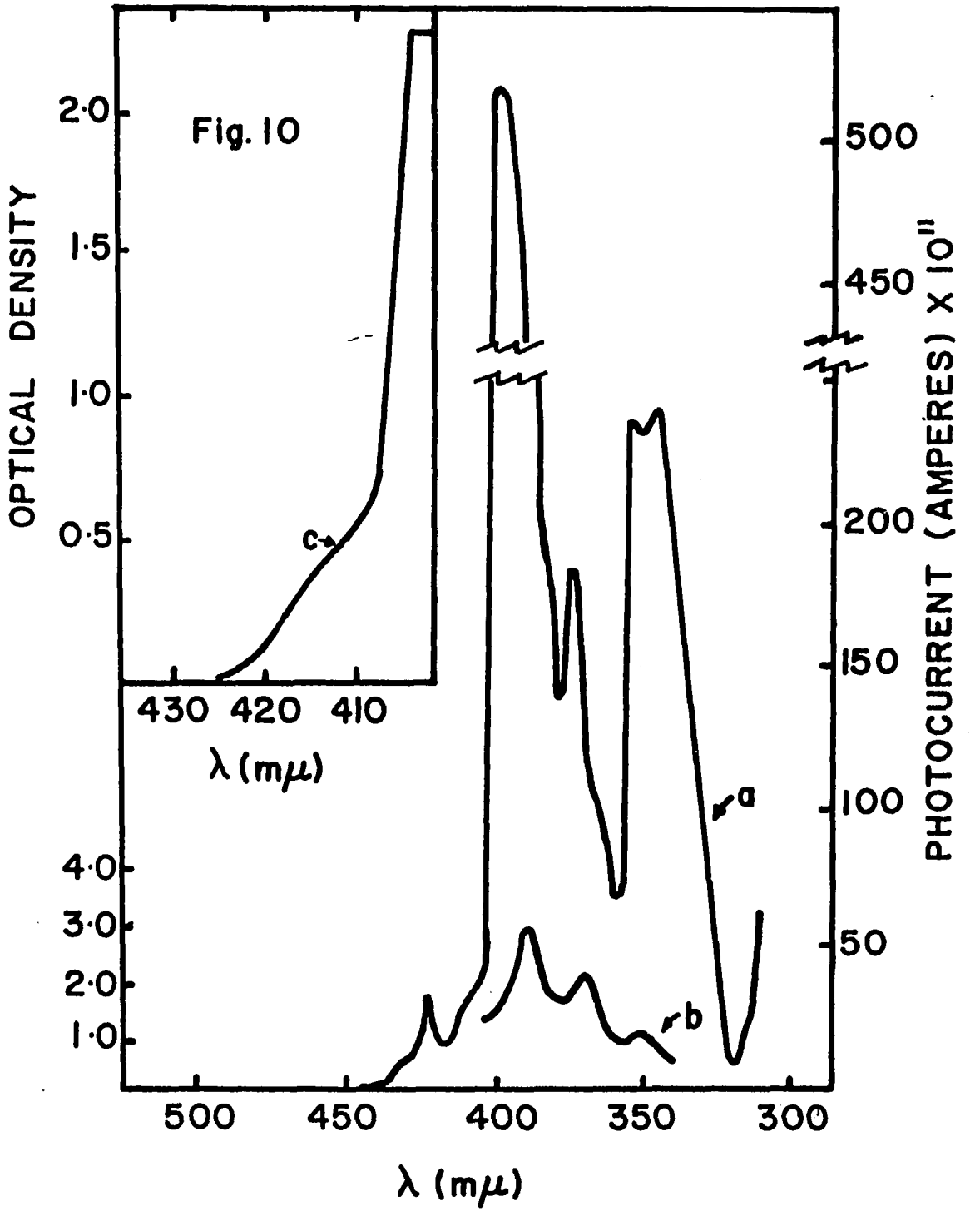
Fig. 10
OPTICAL DENSITY
2·0
1·5
1·0
0·5
4·0
3·0
2·0
1·0
c
430 420 410
λ (mμ)
a
b
500
450
400
350
300
λ (mμ)
500
450
200
150
100
50
PHOTOCURRENT (AMPERES) X 10¹¹

TABLE II

Comparison of Photoconduction and Absorption Peaks

Main Photoconduction Peaks		Crystal Absorption Peaks		Red Shift
Å	(cm^{-1})	Å	(cm^{-1})	(cm^{-1})
4000	(24990)	3931	(25432)	442
3750	(26660)	3725	(26838)	178
3550	(28160)	3529	(28328)	168
3450	(28977)	----	-----	---

current is measured along the surface of the crystal) Lyons[31] and Carswell and Lyons[32] obtained photoconduction action spectra which reproduced the absorption spectrum of the crystal. Furthermore almost all authors find that the photocurrent in surface cells is linear with light intensity.

The above observations are not entirely unexpected; however, the quantitative interpretations of these observations are rather difficult. The discussion will, therefore, be a qualitative one. It is usual to define the steady state excess charge carrier density, $\Delta n(=n_+ - n_+^o = n_- - n_-^o)$ by the equation

$$\Delta n = L\tau \tag{25}$$

when the rate of electron-hole pair generation, L, is uniform throughout the sample and τ is the lifetime of the carriers in the specimen. Let us suppose that the specimen is a rectangular prism with a uniform thickness, d(-2A), between the two opposite plane surfaces, the dimensions of the plane surface being 2B and 2C. Let it further be assumed that a monochromatic radiation is incident normal to one of the plane faces (i. e., the "front surface") and that I_o is the intensity of the incident radiation defined as the number of photons incident on a unit area of the surface per unit time. If I is the intensity in the material and α is the absorption coefficient in reciprocal centimeters, the number of photons absorbed per unit volume per unit time is αI. Thus if η is the quantum efficiency (the number of pairs of free electrons and holes produced per absorbed photon), the rate of generation, L, i. e., the number of electron-hole pairs produced per unit volume per unit time is then equal to $\eta\alpha I$. The quantity, I, is a complicated function of the thickness, d; if d is so small that $\alpha d \ll 1$ there will be interference between the radiation reflected from the front and the back surfaces of the sample if these surfaces are plane and parallel to each other and therefore, the amount of absorbed radiation will

---

[31] L.E. Lyons, J. Chem. Phys. 23, 220 (1955).

[32] D.J. Carswell and L. E. Lyons, J. Chem. Soc., 1734 (1955).

vary rapidly with wavelength. For our purpose, we shall assume that $\alpha d \gg 1$. There being, in this case, no appreciable radiation reflected from the back surface (the surface opposite to the illuminated surface) we may assume that I may be expressed simply by the equation

$$I = I_o(1 - R_o)e^{-\alpha x} \tag{26}$$

where R_o is the reflection coefficient at the surface of an infinitely thick slab and x is the distance from the illuminated surface. Thus the rate of pair production is given by the equation

$$L = \eta\alpha I_o(1 - R_o)e^{-\alpha x} \tag{27}$$

We shall further assume that the lifetime, τ, is defined by the formula:

$$1/\tau = 1/\tau_o + s(1/B + 1/C) \tag{28}$$

which was derived by Shockley.[33] In Eq. (28), τ_o is the bulk lifetime, s is the surface recombination velocity and B and C are the cross-sectional dimensions.

In surface type cells the region between the electrodes is usually uniformly illuminated. From Eq. (18), the rate of surface generation is

$$L_s = \eta\alpha I_o(1 - R_o) \tag{29}$$

and from Eq. (28) if the velocity of surface recombination is large, the lifetime is approximately

$$\tau_s \approx 1/s(1/B + 1/C) \tag{30}$$

where τ_s is now the lifetime of the carriers at the surface. Eq. (25) becomes

$$\Delta n_s = \eta\alpha I_o(1 - R_o)\tau_s \tag{31}$$

---

[33] W. Shockley, "Electrons and Holes in Semiconductors," Van Nostrand, New York (1950) p. 318.

and since, J_{ps}, the surface photocurrent is proportional to Δn_s it is easily seen from Eq. (31) that the photoconduction action spectrum will reproduce the absorption spectrum of the crystal. In the case of a sandwich type cell where most of the current arises from charge carriers moving through the bulk of the material, we need an expression for Δn which takes into account the non-uniformity of the rate of carrier generation as expressed by Eq. (27). According to Smith[34] the excess carrier density is given by the equation

$$\Delta n = [K\tau_o/(\alpha^2\delta^2-1)]\,\langle[(\alpha\delta^2 + s\tau_o)/(\delta + s\tau_o)]\, e^{-x\delta} - e^{-\alpha x}\rangle \qquad (32)$$

and the photocurrent, J_p, is obtained by integrating with respect to x, i. e.

$$J_p = qE(1 + b)\mu_+ W \int_o^\infty \Delta n dx \qquad (33)$$

$$= [q\eta W\delta I_o\tau_o\mu_+(1 + b)(1 - R_o)/(\delta + s\tau_o)]E[1 + (s\tau_o/\delta)/(1 + \alpha\delta)]$$

In eq. (32) and Eq. (33), $K = \eta\alpha I_o\,(1 - R_o)$, q is the electronic charge, W is the width of the sample, δ is the diffusion length of the holes, $b(= \mu_-/\mu_+)$ is the ratio of the electron and hole mobilities and the rest of the symbols are as previously defined. In the limit as $\alpha \to \infty$ the expressions for the current becomes

$$J_{p\infty} = q\eta W\delta I_o\tau_o\mu_+(1 + b)(1 - R_o)E/(\delta + s\tau_o) \qquad (34)$$

J_p may, therefore, be expressed in terms of $J_{p\infty}$ by means of the equation

$$(J_p/J_{p\infty}) = 1 + (s\tau_o/\delta)/(1 + \alpha\delta) \qquad (35)$$

We note that if $s\tau_o \gg \delta$, J_p will increase rapidly as α decreases sufficiently to make $\alpha \approx \delta^{-1}$, the reason being that when $s\tau_o \gg \delta$ the photoproduced carriers will recombine mainly at the surface if they are created at a distance less than δ from the surface, while if they are formed at a distance greater than δ, they will recombine mainly in the

---

[34] R. A. Smith, "Semiconductors," Cambridge University Press (1959) p. 310.

bulk of the crystal and their lifetime will be correspondingly longer. Thus in the case when $\alpha_{\lambda max} > \alpha_{\lambda m} > \alpha_{\lambda \pm}$ where $\alpha_{\lambda max}$ is the absorption coefficient at the peak of the absorption band, $\alpha_{\lambda m}$ is the absorption coefficient which is of the order of δ^{-1} and $\alpha_{\lambda \pm}$ is the absorption coefficient corresponding to some wavelength of excitation on both sides of the absorption peak, we would expect the corresponding structure in the photoconduction action spectrum to be broadened with peaks at wavelengths in the vicinity of $\alpha_{\lambda m}$. These peaks will be separated by a minimum at the wavelength corresponding to λ_{max} in the absorption spectrum when the absorption band is symmetrical about the absorption peak. These deductions appear to suitably explain that particular structure of the photoconduction action spectrum which corresponds to the absorption peak at 352.9mμ in Fig. 10. We note that the structure is split, peaking at 355 and 340 mμ and the minimum between the two peaks coincides with the maximum of the absorption peak. The structures of the photoconduction action spectrum in the wavelength range, 400 mμ ≥ λ ≥ 360 mμ are all shifted towards the red with respect to the corresponding structures in the absorption spectrum. It may accordingly be concluded that the free carrier density resulting from excitation with light within this wavelength range, will be limited mainly by the rate of recombination at the surface. In accord with the linear dependence of the photocurrent on light intensity (see Table I for λ = 390 mμ) it may be concluded (provided that the surface recombination is "bimolecular") that charge carrier generation at the surface is biphotonic.

The photocurrent for λ = 420 mμ is approximately proportional to the square root of light intensity. It is, however, doubtful that the process of carrier generation resulting from excitation with monochromatic light at 420 mμ is intrinsic (i. e., electron-hole pairs are produced by the excitation of the host crystal). The leading edge on the long-wavelength side of the absorption spectrum of an anthracene sandwich cell shown in Fig. 10c shows a hump between 420 and 410 mμ. This hump may be due to the presence of impurities. The impurity mole-

cules were probably anthraquinone and/or naphthacene molecules; the former could have been formed from the oxidation of anthracene in the process of melting during the preparation of the sandwich cell. The photoconduction peak at 425 mμ probably corresponds to this hump. Kommandeur also found a photoconduction peak at 425 mμ for crystals which were 1 to 4 mm thick but only when the illumination was made through the negative electrode.[35] The relatively poor resolution of the photoconduction peaks when the illuminated side was positive compared to the resolution of the peaks when the side illuminated was negative and which may be deduced from Fig. 20 of his dissertation is probably the more correct explanation of why the 425 mμ peak was not detected during his experiments when the cell was illuminated through the positive electrode. The photoconduction action spectrum depicted in Fig. 10a was obtained from a 30 μ thick crystal of anthracene when the illuminated side was positive. The better resolution of the photoconduction peaks is largely due to the greater gain in sensitivity which is realizable for thinner crystals, the gain being inversely proportional to the thickness of the photoconductive material. It is not, however, uncommon to find structures in the photoconduction action spectrum at wavelengths which appear to be beyond the long-wavelength edge of the crystal absorption spectrum. Similar structures are evident in the photoconduction action spectrum of rubrene and tetraphenylbutadiene.

The photoconduction action spectrum of rubrene is shown in Fig. 11a and b. Fig. 11a shows the photoconduction, fluorescence and absorption spectra associated with the first electronic transition while those corresponding to the higher electronic transitions are shown in Fig. 11b. The photoconduction action spectrum of rubrene was taken from two directions; one coming from the red and going toward the blue and the other in the reverse direction. The analysis of the spectrum is shown in Table III. A structure is called apparent if it is displaced from its previous position and real if no displacement is

---

[35] Kommandeur, op. cit.

Fig. 11. (a) Photoconduction Action Spectrum of Rubrene and Its Fluorescence and Absorption Spectra

(b) Photoconduction Action and Absorption Spectra Associated With Higher Electronic Transitions

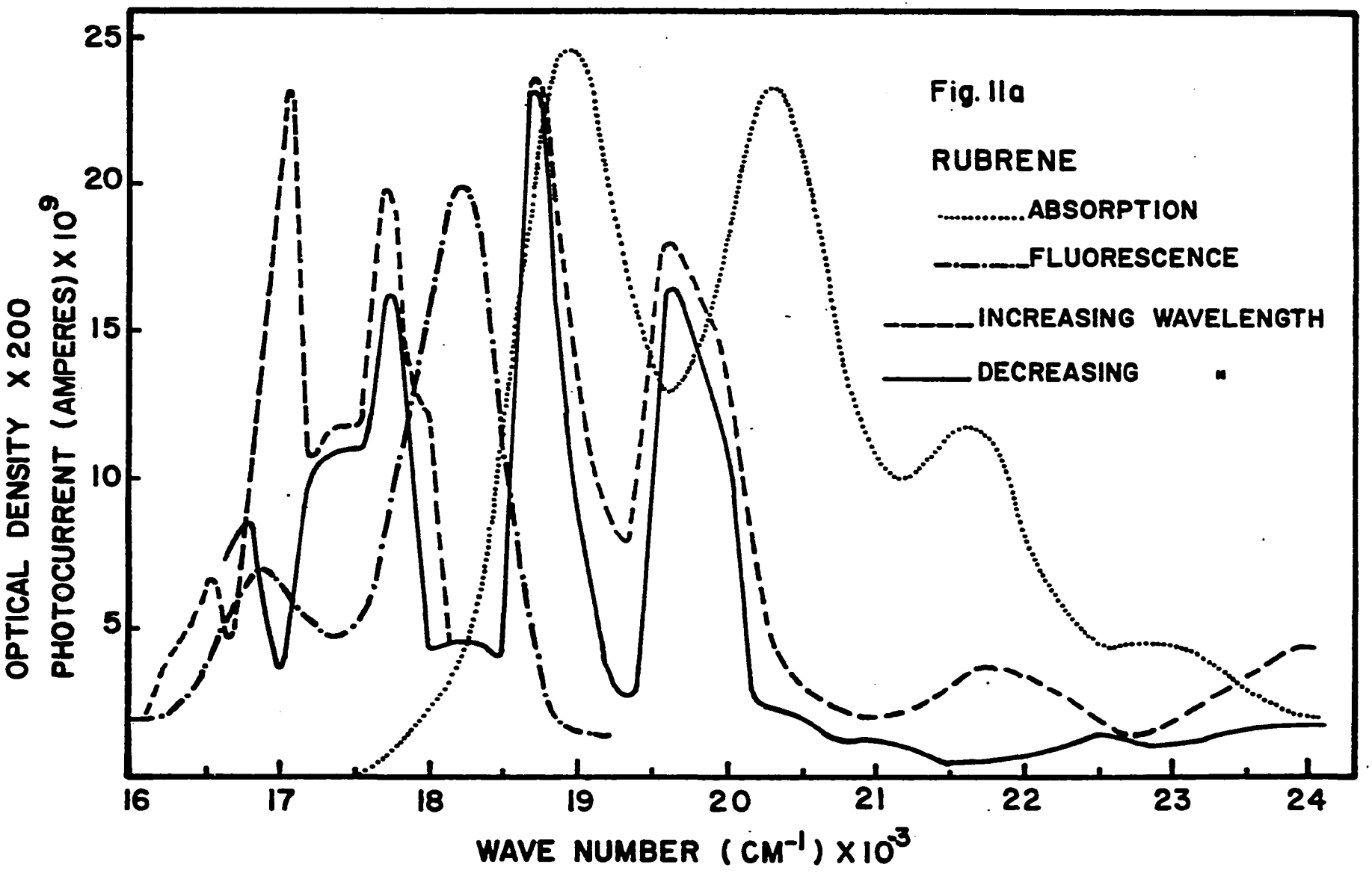
Fig. IIa
RUBRENE
ABSORPTION
FLUORESCENCE
INCREASING WAVELENGTH
DECREASING
OPTICAL DENSITY X 200
PHOTOCURRENT (AMPERES) X 10^9
25
20
15
10
5
16
17
18
19
20
21
22
23
24
WAVE NUMBER (CM^-1) X 10^3

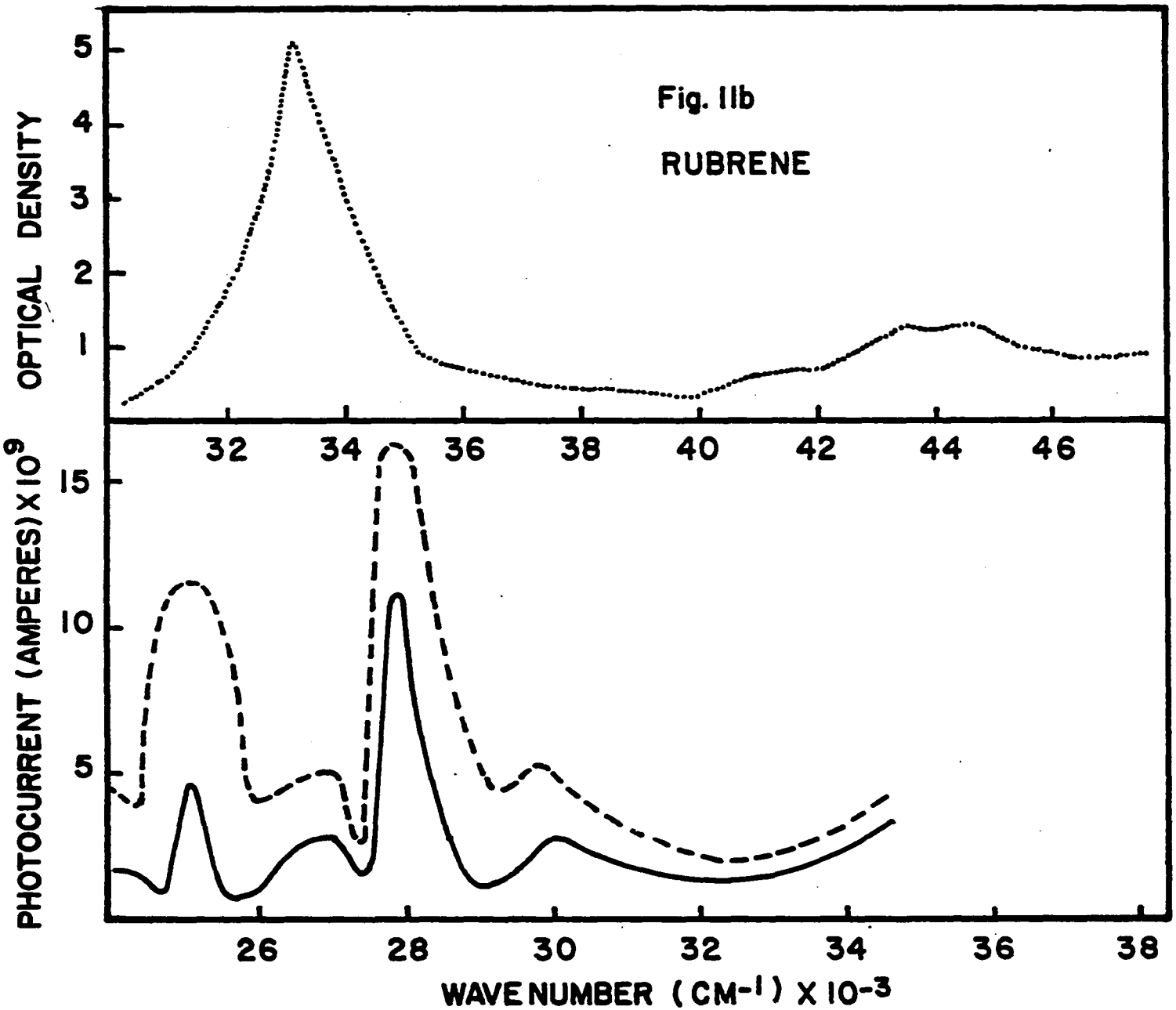
Fig. IIb
RUBRENE
OPTICAL DENSITY
5
4
3
2
1
32
34
36
38
40
42
44
46
PHOTOCURRENT (AMPERES) X 10^9
15
10
5
26
28
30
32
34
36
38
WAVE NUMBER (CM-1) X 10-3

TABLE III

Structures in the Action Spectrum of Rubrene

ν cm^{-1}	Description	Remarks
16.540	peak	apparent
16,800	peak	apparent
17,098	peak	reverses
17,760 ± 50	peak	real
17,400	shoulder	real
18,160	plateau	real
18,720 ± 50	peak	real
19,640 ± 50	peak	real
20,400	shoulder	doubtful
21,740	hump	apparent
24,000	hump	real
25,080 ± 100	peak	real
27,000 ± 100	hump	real
27,880 ± 100	peak	real
29,840	hump	real

observed. Correspondence between the real peaks and those of the absorption spectrum is shown in Table IV with the graphically calculated red shifts. It is noted that the real photoconductive peaks in Fig. 11a are displaced toward the red by approximately 1500 cm^{-1} with respect to the main absorption band of the material in solution. The structures of the photoconduction spectrum in Fig. 11b which presumably are associated with the excitation of higher electronic states are shifted approximately by 6000 cm^{-1}. Red shifts of this order in the absorption spectrum of organic substances in going from solution to crystal are not unreasonable. There is a very striking similarity between the apparent structures of the photoconduction action spectrum below 17,500 cm^{-1} and the fluorescence spectrum. The apparent peaks at 16,540 and 16,800 cm^{-1} seem to be related to the fluorescence peaks at 16,944 and 18,210 cm^{-1}. The absorption and fluorescence peaks are shown in Table V. It is also interesting to note that the photoconduction action spectrum is significantly enhanced and broadened when the action spectrum is determined by varying the wavelength of the exciting radiation from shorter to longer wavelengths.

In Fig. 12 are shown the photoconduction action spectrum of a 40 micron thick crystal of tetraphenylbutadiene and the absorption spectrum of the material in solution in n-hexane. While there are no structures observable in the solution spectrum, there appears a large number of structures in the photoconduction action spectrum. The splitting of the main photoconduction band (i. e., the one between 24,750 - 35,000 cm^{-1}) is probably due to the effect of a large rate of surface recombination which was previously discussed in connection with the photoconduction peak in the anthracene photoconduction spectrum. If this were the case the absorption maximum of tetraphenylbutadiene in the crystalline state will be located at 27,450 cm^{-1}. Since the absorption maximum in solution is at 29,087 cm^{-1} this would represent a red shift of 1,637 cm^{-1} of the absorption peak in going from solution to the crystalline state. The photoconduction peaks at 22,200 and 24,100 cm^{-1} are probably due to the presence of impurity in the crystal.

TABLE IV

Postulated Correspondence of Peaks in Rubrene

Solution Spectrum (cm^{-1})	Action Spectrum (cm^{-1})	Red Shift (cm^{-1})
18,934	17,760 ± 50	1,174 ± 50
20,278	18,720 ± 50	1,558 ± 50
21,639	19,640 ± 50	1,599 ± 50
22,825	hump from 20,400 to 21,500	~ 2,425
	24,000	
	25,080 ± 100	
33,103	27,000 ± 100	~ 6,000
	27,880 ± 100	
	29,840	

TABLE V

Absorption and Fluorescence Peaks of Rubrene in Solution

Solvent:	Cyclohexane	E. P. A.
Temperature:	Room Temperature	77°K
	Absorption Peaks (cm^{-1})	Fluorescence Peaks (cm^{-1})
	18,934	18,210
	20,278	16,944
	21,639	15,694
	22,825	
	33,103	
	44,234	

Fig. 12. Photoconduction Action Spectrum of Tetraphenylbutadiene

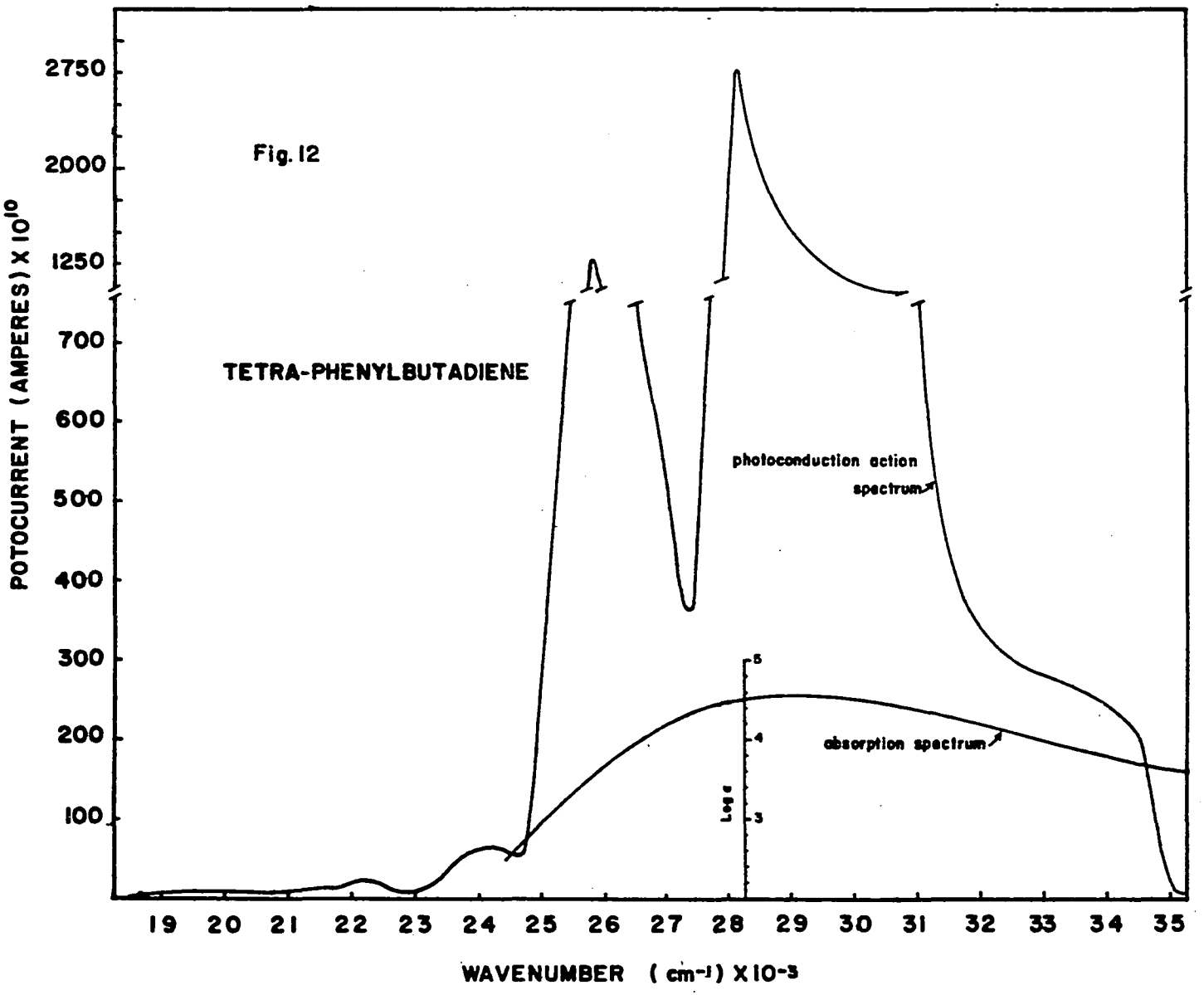
Fig. 12
TETRA-PHENYLBUTADIENE
photoconduction action spectrum
absorption spectrum
POTOCURRENT (AMPERES) X 10^10
2750
2000
1250
700
600
500
400
300
200
100
Log ε
5
4
3
19 20 21 22 23 24 25 26 27 28 29 30 31 32 33 34 35
WAVENUMBER (cm^-1) X10^-3

CHAPTER IV

PHOTOCONDUCTION UNDER PULSED ILLUMINATION

A pulse technique which was first used successfully by Yamakawa[1] for measuring mobilities of charge carriers and which will be referred to as the "crystal conductivity counter method" was utilized primarily for the measurement of drift mobilities of holes, μ_+, and electrons, μ_-, in sandwich cells of anthracene and tetraphenylbutadiene. In addition, the method was used also to evaluate charge carrier lifetime and quantum yields, and to study the variation of photocurrent with voltage, light intensity, wavelength of incident light and temperature.

A. Principle of the Method

The crystal is mounted in a sandwich arrangement between two parallel electrode plates, one (or both) of which is (are) transparent, and a collecting voltage is applied to a series combination of a resistor and the crystal. A short pulse of strongly absorbed radiation strikes the transparent electrode and generates charge carriers at the crystal surface; these carriers are then displaced by the electric field. This displacement of carriers induces a charge on the electrodes and the resulting voltage pulse is amplified and displayed on an oscilloscope. The time constant of the output circuit is made large compared with the duration of the photoconductive transient so that the circuit acts as an integrator. A schematic diagram of this circuit is given in Fig. 13. A collecting voltage, V_c, is applied across the crystal. The capacitance C_T represents the combined capacity of crystal, leads, preamplifier input, etc. The charge carriers generated at the irradiated surface are drawn into the bulk, thus inducing a charge q on the electrodes. Under conditions of large input time constant, a corresponding voltage pulse $v = q/C_T$ is produced at the amplifier input.

---

[1] K. A. Yamakawa, Phys. Rev., 82, 522 (1951).

Fig. 13. Schematic of Arrangement Used in the Study of Pulsed Photoconductivity.

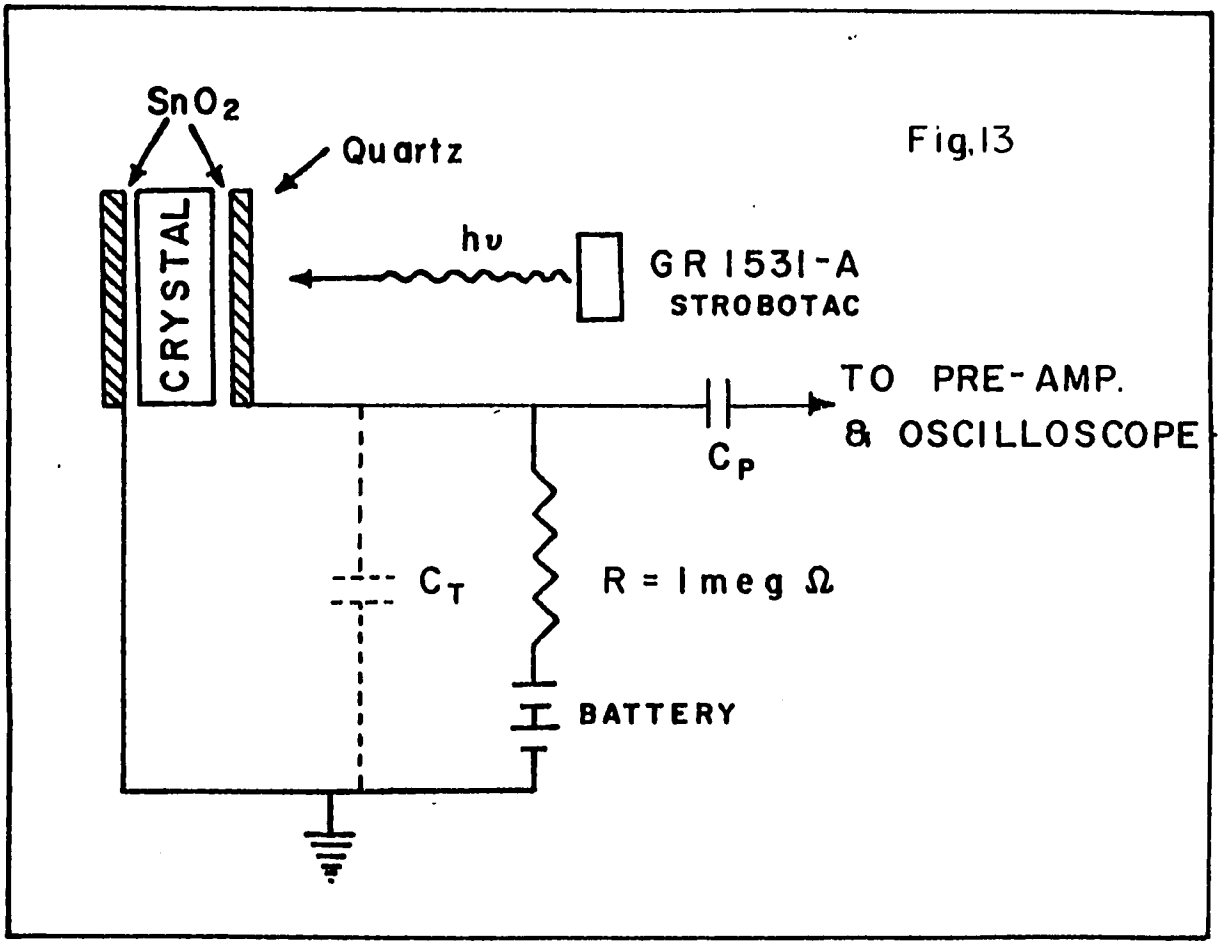
SnO2
Quartz
CRYSTAL
hν
GR 1531-A
STROBOTAC
TO PRE-AMP.
& OSCILLOSCOPE
CP
CT
R = 1meg Ω
BATTERY

Fig.13

The time dependence of the charge pulse q(t) is derived by making the following assumptions:

(1) that n_0 charge carrier pairs are generated instantaneously at time t = 0 at the illuminated surface very near the electrode, x = 0;

(2) that a uniform electric field $E = V_c/d$ exists in the crystal where d is the crystal thickness; and

(3) that there is a uniform density of traps throughout the crystal giving rise to an average time $\tau = (\sigma\bar{v}N_t)^{-1}$ before trapping; σ is the trapping cross-section, $\bar{v}$ is the average carrier velocity and N_t is the trap density. The average distance the charge carriers drift before trapping (Schubweg, ω) is given by $\omega = \mu E\tau$ where μ is the mobility of the charge carrier.

With these assumptions we may write

$$q(t) = (n_0 e\omega/d)(1-\exp[-\mu Et/\omega]) \tag{36}$$

which is applicable for times $t \leq d/\mu E$. This can be rewritten as

$$q(t) = (n_0 eE\mu\tau/d)(1-\exp[-t/\tau]) \tag{37}$$

For times greater than $d/\mu E$

$$Q = (n_0 e\omega/d)(1-\exp[-d/\omega) \tag{38}$$

For the case that τ is very large compared to t, Eq. (37) becomes

$$q(t) = n_0 e\mu Et/d \tag{39}$$

Hence, the charge pulse has an approximately linear rise until a time $t_{tr} = d/\mu E$ corresponding to the collection of n_0 charge carriers. The measurement of the time t_{tr} allows one to compute the drift mobility from the relation

$$\mu = d/Et_{tr} \tag{40}$$

Even if trapping is important, a break or discontinuity occurs at time t_{tr} provided only that a fraction of the charge carriers reach

the counter electrode. Using sensitive electronic detection instruments, the transit time can be accurately determined. Thus the analysis of the pulse shapes leads to values of the drift mobility, and may yield lifetimes of charge carriers from which the quantum yield may be evaluated and the kinetics of photocurrent generation studied.

In order to analyze the pulses Eq. (36) is rewritten as follows:

$$v_t = n_0 e\tau/C_T t_{tr} \begin{cases} (1-\exp[-t/\tau]), & t<t_{tr} \\ (1-\exp[-t_{tr}/\tau), & t>t_{tr} \end{cases} \tag{41}$$

In practice, however, this has to be modified because the excitation is not instantaneous and the flash has a finite tail. This aspect has been discussed in detail by Michel.[2] From the equations given above it can be seen that the dependence of the pulse height on the applied field gives a measure of the Schubweg per unit field, ω_0. In the simple trapping model $\omega_0 = \mu\tau$, and a method is provided for lifetime evaluations. Alternatively, this gives an independent check on μ if τ is known. The peak pulse height v_S is given by

$$v_S = AV(1-\exp[-d^2/\omega_0 V]) \tag{42}$$

where A is a constant independent of V, the applied voltage across the crystal. Eq. (42) predicts that v_S will be linear with voltage for low voltages and will saturate at high voltages.[3] This voltaic behavior of v_S will be referred to as"Hecht behavior." If the range can be determined from saturation data wherein it can be assumed that essentially all of the charge carriers produced are pulled through the crystal, it is possible to compute the quantum efficiency, η, defined as the number of conduction charge carriers released into bulk per absorbed quantum.

---

[2]A. E. Michel, Phys. Rev., 121, 968 (1961).

[3]K. Hecht, Z. Physik, 77, 235 (1932).

B. Experimental

Fig. 13 gives the schematic diagram of the electronic arrangement used to study the transient photoconductivity in organic crystals. The samples for study were prepared as described previously. The crystals were illuminated using two different light sources. A modified G. R. type 1531A Strobotac having a flash duration of 1.5 μsec and a total photon output of 2.2×10^9 per flash centered at 402 mμ was used for carrier generation with strongly absorbed light. For the study of transients with weakly absorbed light, an Edgerton, Germeshausen and Grier, Inc., Microflash unit, model 549, with a flash lifetime of 0.57 μsec and an output of 7 joules per flash was used. Suitable Corning glass filters were used to limit the wavelength of the incident light on the crystal. A Perkin-Elmer Universal Monochromator, Model 83 with quartz prism, was employed in the study of photoconductivity action spectra. The effects of wavelength and intensity of illumination were studied using appropriate combinations of Corning glass, neutral optical density screens and the above monochromator. The detection instruments consisted of the Tektronix 545A oscilloscope with type H and type D plug-in units and the Tektronix 585 oscilloscope with type 80 and type 82 preamplifiers and their associated accessories as well as the type 81 adapter in conjunction with the lettered series of Tektronix amplifiers for the measurement of signals of lesser intensities. The capacitances were measured with a G. R. 1650 Impedance Bridge.

The photon output of the G. R. 1531A Strobotac was calculated from the integrated output of a 1P28 photomultiplier tube. The gain of the tube was measured and found to be 2.5×10^4 at an operating voltage of 1130 volts. The photo-cathode efficiency was 17% for the range of 300-400 mμ. The total photon output was computed from

$$(100/17)(CV_{max}/e)(1/G) \qquad (43)$$

where C = total capacitance, V_{max} = total pulse height in volts, e = electronic charge in coulombs and G = gain of the phototube.

The temperature dependent measurements were made using a modified conduction chamber enclosed in a Precision Scientific oven provided with a quartz window and a thermostatic control. The temperature of the cell was read from a thermistor in contact with the cell.

The anthracene was Eastman H480 from Eastman Organic Chemicals, Rochester 3, New York. Anthracene grown from a melt which is squashed between two quartz plates usually crystallizes with its 001 face parallel to the quartz surfaces. Consequently, mobilities quoted herein are in a direction perpendicular to the 001 face.

C. Results and Discussion

It is necessary to make a few preliminary remarks:

(1) A total of 25 anthracene cells have been studied. Only those results characteristic of the greater majority of cells made will be presented, and then only for cells whose behavior is "average."

(2) The study will concern itself primarily with the majority carriers (i. e., holes).

(3) It will be assumed that the penetration of photons into the bulk of the crystal is very slight, or negligible, compared to the thickness d.

If one assumes the simple trapping model discussed earlier, it can be seen that the pulse shape will be described by Eq. (41). A set of oscilloscope traces for various applied voltages is reproduced in Fig. 14. In the case of various cells, C_T varied from 200 - 300 $\mu\mu$F. An examination of the pulses shows that the shapes are in accord with theory only to a first approximation. This tail can be attributed to a detrapping process due to the presence of shallow traps. These traps are supposed to retain carriers for a short period after the time of transit of the majority of the carriers and then release them into the valence band giving rise to delayed collection at the counter electrode. In the present instance the pulses show a sharp linear rise only at very low fields. At higher voltages the photocurrent pulses tail off making it difficult to determine the transit time. Moreover, the variation of

Fig. 14. Photocurrent pulses in anthracene - cell XXII. The Strobotac light pulse is dotted in at left. The capacitance C_T was 269 pf. Irradiation was effected through Corning Filter C. S. 7-60; no monochromator was used.

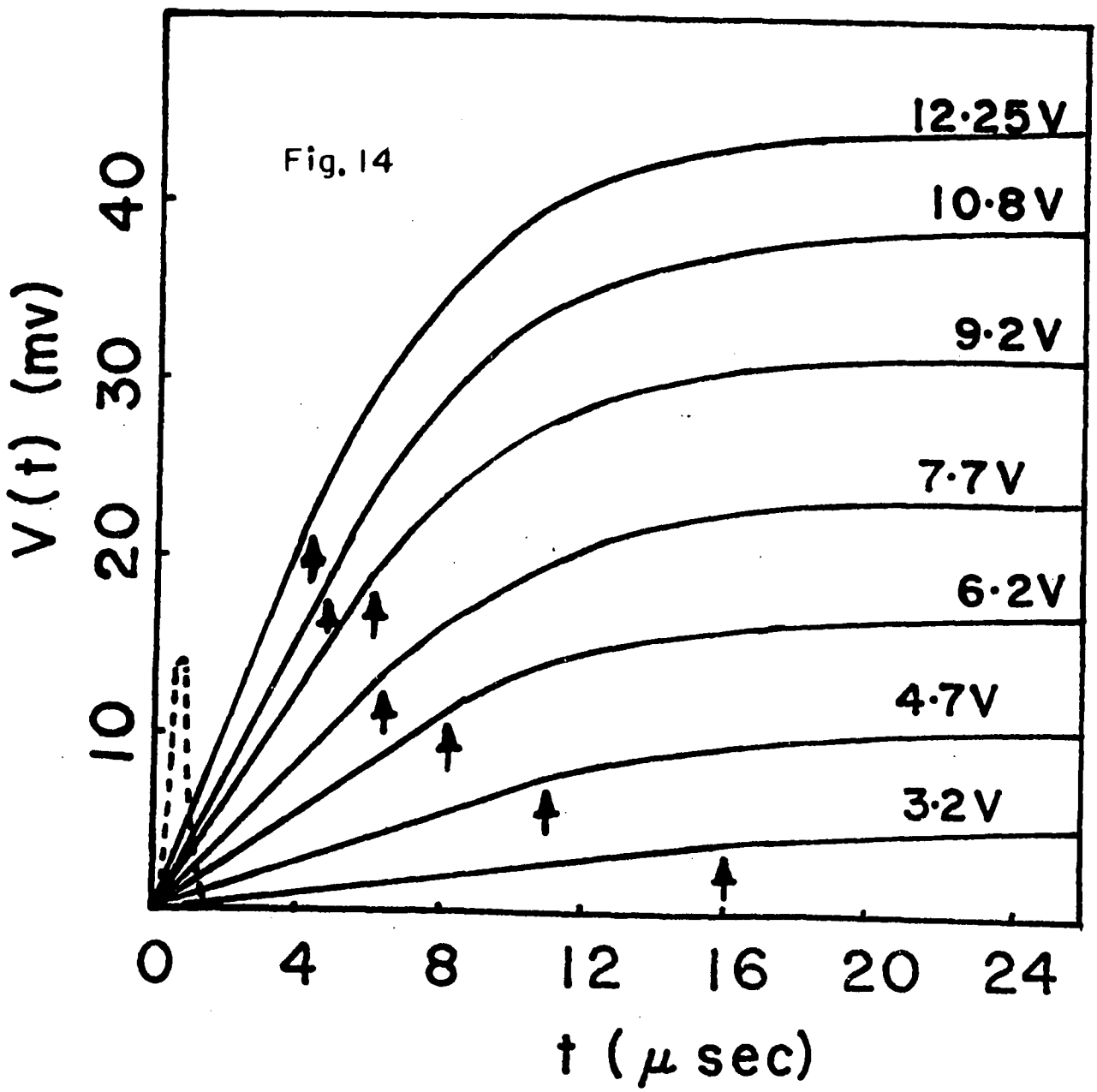
Fig. 14
12·25V
10·8V
9·2V
7·7V
6·2V
4·7V
3·2V
V(t) (mv)
10
20
30
40
0
4
8
12
16
20
24
t (μ sec)

pulse height with applied field does not follow Hecht's equation. In spite of these anomalies one can still arrive at valid conclusions with regard to transport parameters if one analyzes only the leading linear edge of the pulses and analyzes these only at low electric field strengths.

C-1. Mobility of Holes

The transit times t_{tr} of holes were computed for different applied voltages as indicated in Fig. 14. It can be seen that as the voltage is increased it becomes more and more difficult to locate the discontinuity in the curves. The arrow marks indicate the value of t_{tr}. The mobility μ is then calculated by obtaining the slope of the plot of $1/t_{tr}$ vs. V as follows:

$$\partial V/\partial(1/t_{tr}) = d^2/\mu \tag{44}$$

Fig. 15 gives such an evaluation. The values of mobility obtained from several experiments are given in Table VI. That the value is quite consistent with those reported in the literature can be seen from Table VII. Further, the fact that the transit times measured by adopting this model have yielded reproducible and reasonable values of μ indicates that the analysis of same is correct.

C-2. Thermal Dependence of Mobility

The effect of temperature on mobility was studied. The results are given in Fig. 16 and Table VIII. The curve obtained fits the equation

$$\mu = AT^{-x} \tag{45}$$

(where A is a constant) which is characteristic of scattering by acoustical lattice vibrations when $x = 1.5$. However, the temperature range is small and so the above equation is only approximately validated.

Fig. 15. Reciprocal transit time t_{tr} vs. applied voltage V - cell XXII. Thickness of cell was d = 9.29×10^{-3}cm. The slope of the straight line is d^2/μ and μ is found to be 1.5 cm^2/v.sec.

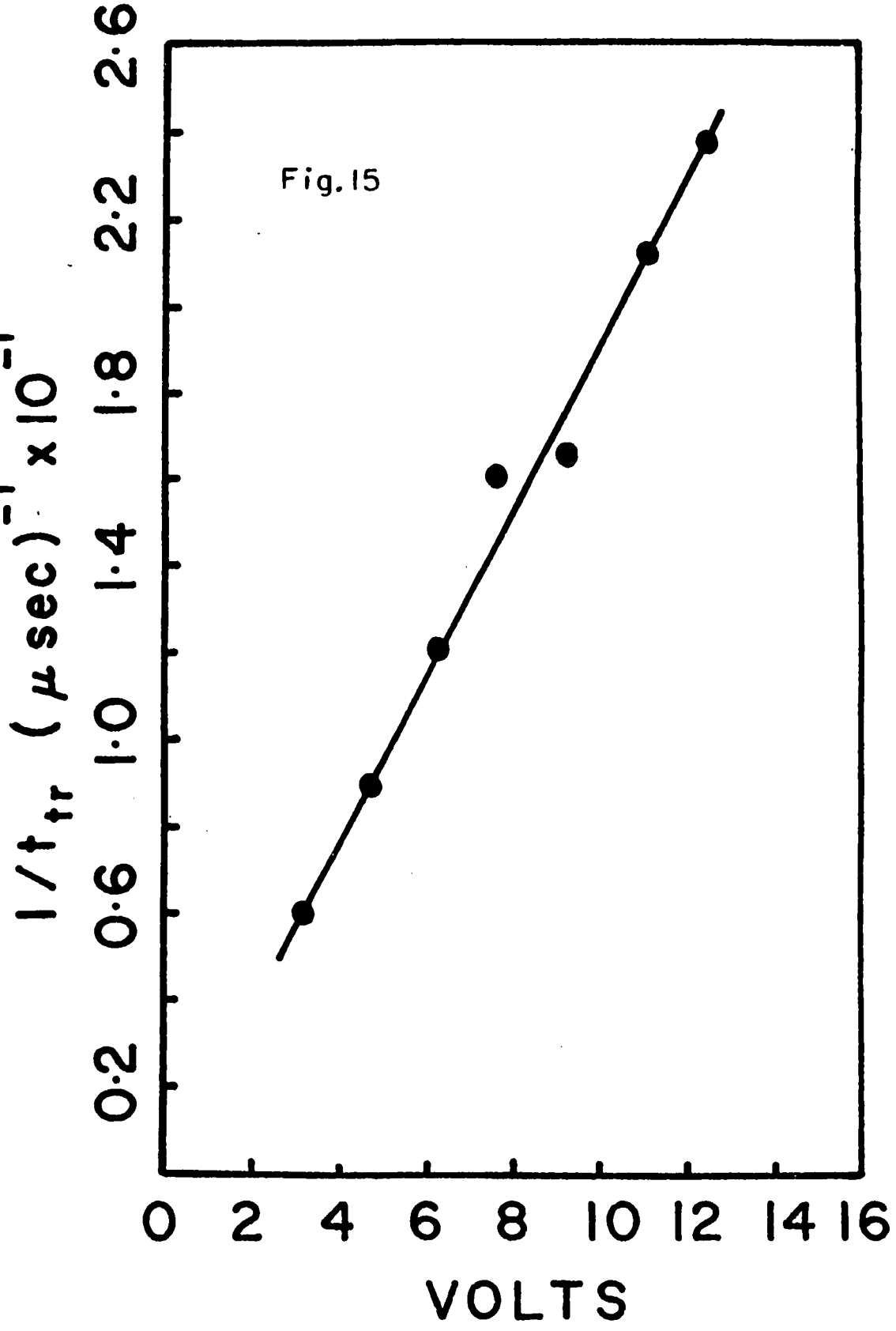
Fig. 15
$1/t_{tr}$ (μsec)$^{-1}$ x 10^{-1}
0·2
0·6
1·0
1·4
1·8
2·2
2·6
0
2
4
6
8
10
12
14
16
VOLTS

Fig. 16. Log μ_+ vs. log T for cell XIII. Applied voltage was V = 6 v. Slope is 1.83.

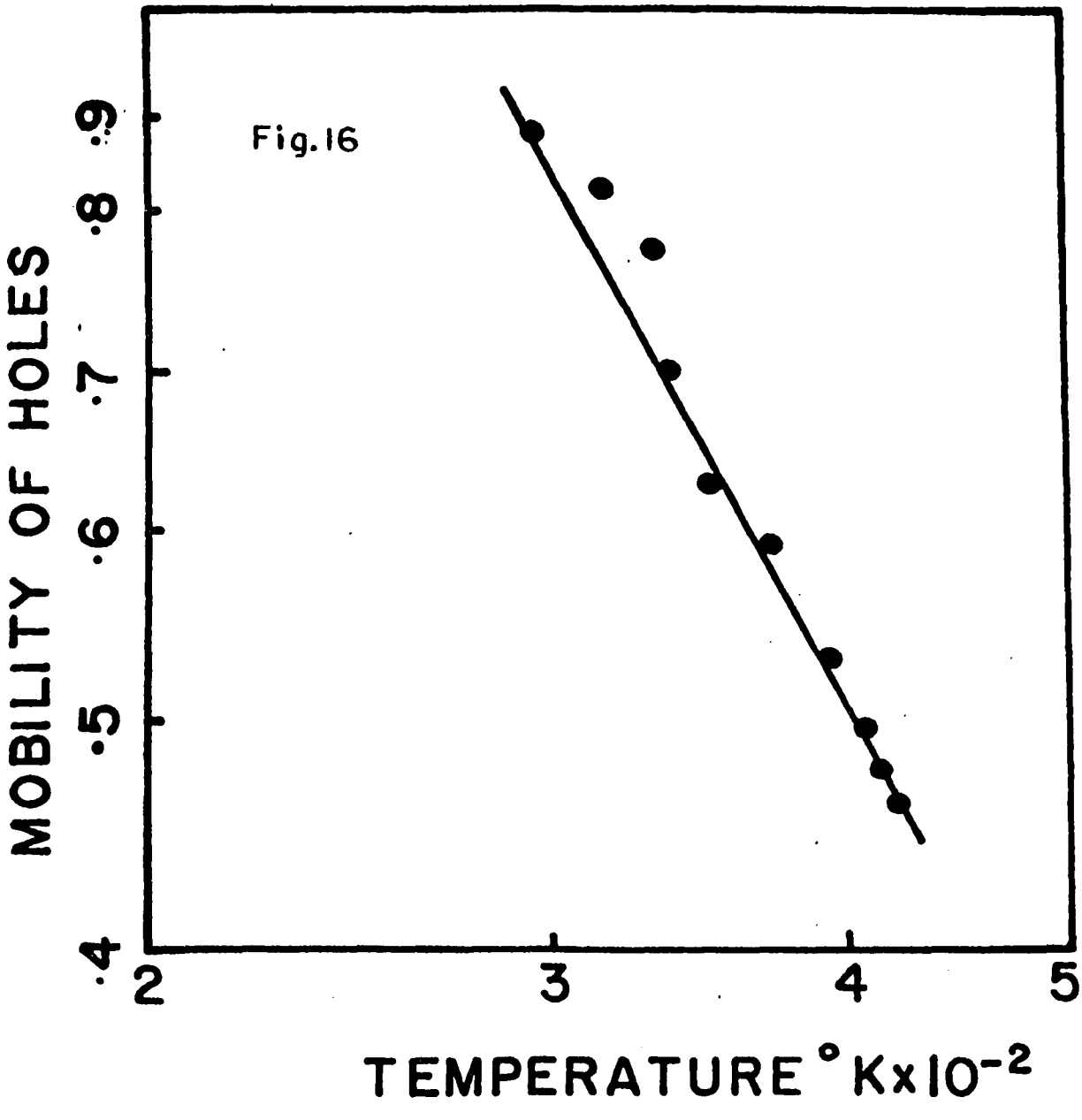
Fig.16
MOBILITY OF HOLES
.9
.8
.7
.6
.5
.4
2
3
4
5
TEMPERATURE °K x 10⁻²

TABLE VI

Mobility of Holes in Anthracene

($22^{\circ}C$, and Strobotac Illumination)

Cell	d($\times 10^{-4}$cm)	Slope	μ(cm^2/V sec)
XIII	62.8	5.04×10^{-5}	0.783
XI	68.2	3.98×10^{-5}	1.17
IX	67.9	5.5×10^{-5}	0.838
V	53.3	6.28×10^{-5}	0.452
VIII	59.0	4.76×10^{-5}	0.73
III	46.4	4.42×10^{-5}	0.487
IV	49.0	3.0×10^{-5}	0.800[a]
XXII	92.9	5.8×10^{-5}	1.5
XIII	62.8	4.4×10^{-5}	0.896[b]

a) Slope indefinite due to scattering of points.

b) Using Microflash.

TABLE VII

Mobility of Holes - Anthracene

Author(s)	μ_+ (cm^2/V sec)
Kepler[4]	0.4 - 2
LeBlanc[5]	0.95
Helfrich and Mark[6]	0.43 ± 0.05
Boroffka[7]	2.3
Raman and McGlynn[8]	0.48
Present data	0.45 - 1.5

[4] Phys. Rev., 119, 1226 (1960).
[5] J. Chem. Phys., 33, 626 (1960).
[6] Z. Physik., 166, 370 (1962).
[7] Ibid., 160, 93 (1960).
[8] J. Chem. Phys., 40, 515 (1964).

TABLE VIII

Variation of μ with Temperature

(Temperature Range: $22^{\circ}C$ to $160^{\circ}C$)

Cell	d (in μ)	Voltage	x
X	68.4	6	1.73
XIII	62.8	6	1.83
VIII	59.0	6	1.46
XVI	60.4	5	2.30

C-3. Mean-Free Lifetime and Range

Attempts were made to evaluate the mean-free time τ and Schubweg ω. Unfortunately, the pulse height vs. applied voltage curve does not follow a true Hecht behavior and consequently no estimate of ω could be obtained. Theoretically, the lifetime τ can be measured directly from the pulse shape at low fields. By choosing three equally spaced points t_1, t_2, and t_3 in the time interval $t' \leq t \leq t_{tr}$, where t' is flash duration, and measuring the corresponding voltages v_1, v_2, and v_3 the lifetime can be calculated from

$$(v_3-v_2)/(v_2-v_1) = \exp(-[t_2-t_1]/\tau) \qquad (46)$$

Since the crystals did not exhibit low-voltage unsaturation, the equation could not be applied. However, a rough estimate was made by analyzing some of the pulses which exhibited slight curvature. Values of τ between 10^{-4} and 10^{-5} sec were obtained.

If one assumes that the lifetime is 5 to 10 times greater than the longest transit time measured, then a value of 8×10^{-5} sec - 16×10^{-5} sec is obtained. This yields a value of 12×10^{-5} $cm^2/V.$ for ω_0 if μ is taken as 1 $cm^2/V.$ sec. This value would appear to be reasonable. In view of the above difficulties it was not possible to study the effect of temperature and voltage on τ.

C-4. Temperature Dependence of Carrier Population

Fig. 17 shows the variation of pulse height with reciprocal temperature in a semi-log plot. The slope gives an activation energy of $\Delta E = 0.14$ ev. which agrees reasonably well with values reported from D. C. measurements (~0.17 ev).[9] It is not improper to conclude that the increase in D. C. photocurrent with temperature is due to increase in carrier population, as has long been supposed.

---

[9] D. M. J. Compton, W. G. Schneider and T. C. Waddington, J. Chem. Phys., 27, 160 (1957).

Fig. 17. Log pulse height vs. 1/T for cell XIII. Applied voltage was 6 v. Thickness was 6.28×10^{-3} cm. ΔE was found to be 0.14 ev.

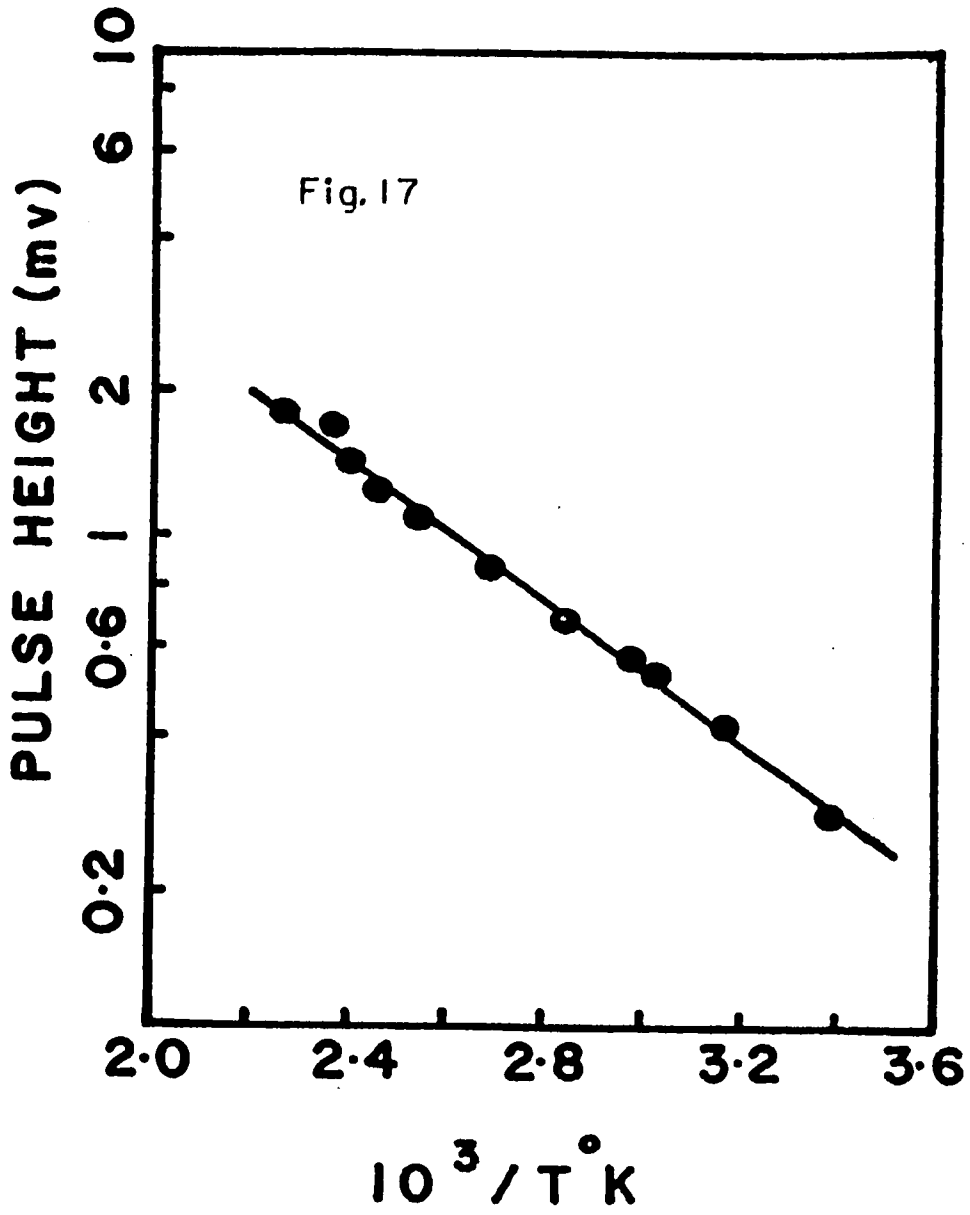
Fig. 17
PULSE HEIGHT (mv)
10
6
2
1
0·6
0·2
2·0
2·4
2·8
3·2
3·6
10 3 / T °K

C-5. Spectral Dependence of Carrier Population

Fig. 18 depicts a photoconduction action spectrum which represents the dependence of carrier population on excitation wavelength. Lamp output has been normalized to a constant photon number and the ordinate is proportional to a quantum efficiency.

The photoconductivity action spectrum is in qualitative agreement with the crystal absorption spectrum of Craig and Hobbins.[10] It differs from the one obtained by Kepler[11] in that the first photoconduction peak is somewhat shifted towards longer wavelengths and shows no further significant structure. The quantum efficiency for strongly absorbed light is relatively less than that for weakly absorbed light indicating that the lifetimes of charge carriers generated closer to the surface are relatively shorter than those generated in the bulk

C-6. Intensity Dependence of Carrier Population

In Fig. 19 the pulse height is plotted against relative intensity of illumination for different voltages with strongly absorbed light. The linearity indicates that the photogeneration is a first order process with respect to light intensity. The experiments were repeated with weakly absorbed light and the results were similar.

C-7. Pulse Shape at Longer Times

It is observed that the pulses have long tails (see, for example, Fig. 14) and it seems appropriate to inquire into the origin of this slow approach to pulse saturation. The interpretation which we consider most likely involves a delayed depopulation of surface traps, and we shall deal with this first. In our zeroth order treatment of transport parameters which has previously been given (vide supra), the fact that the pulses show considerable tailing was neglected altogether. The successful conclusions that were thereby derived justify such neglect.

---

[10] D. P. Craig and P. C. Hobbins, J. Chem. Soc., 2309 (1955).

[11] R. G. Kepler, op. cit., vol. 119, p. 1226.

Fig. 18. Photoconductivity action spectrum for anthracene - cell XXI. Thickness d = 3.43×10^{-3} cm; applied voltage was V = 23 v.

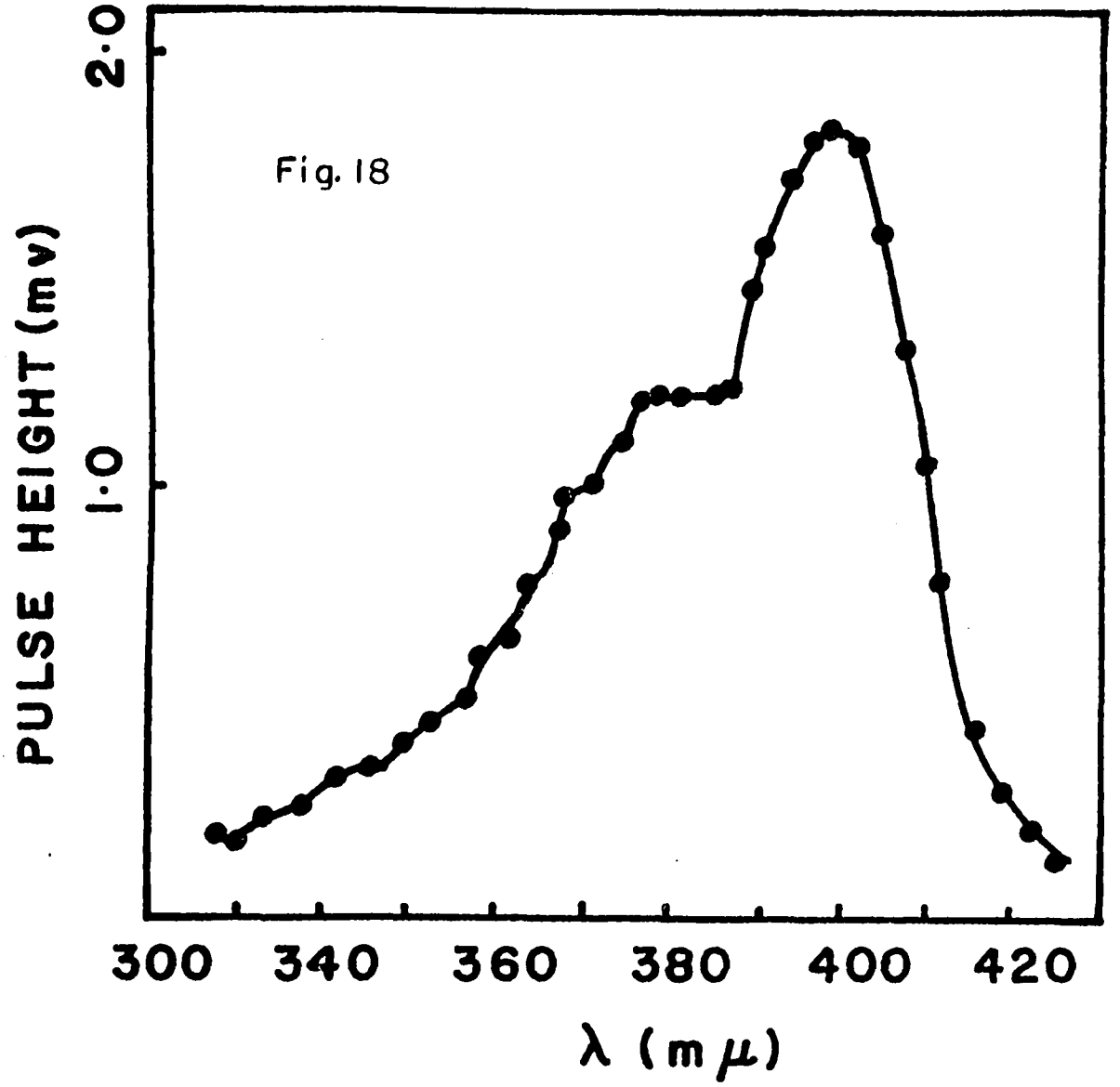
Fig. 18
PULSE HEIGHT (mv)
2·0
1·0
300
340
360
380
400
420
λ (mμ)

Fig. 19. Pulse height vs. percent light intensity. Anthracene - cell XXII. Irradiation was through Corning filter C. S. 7 - 60.

Fig. 19

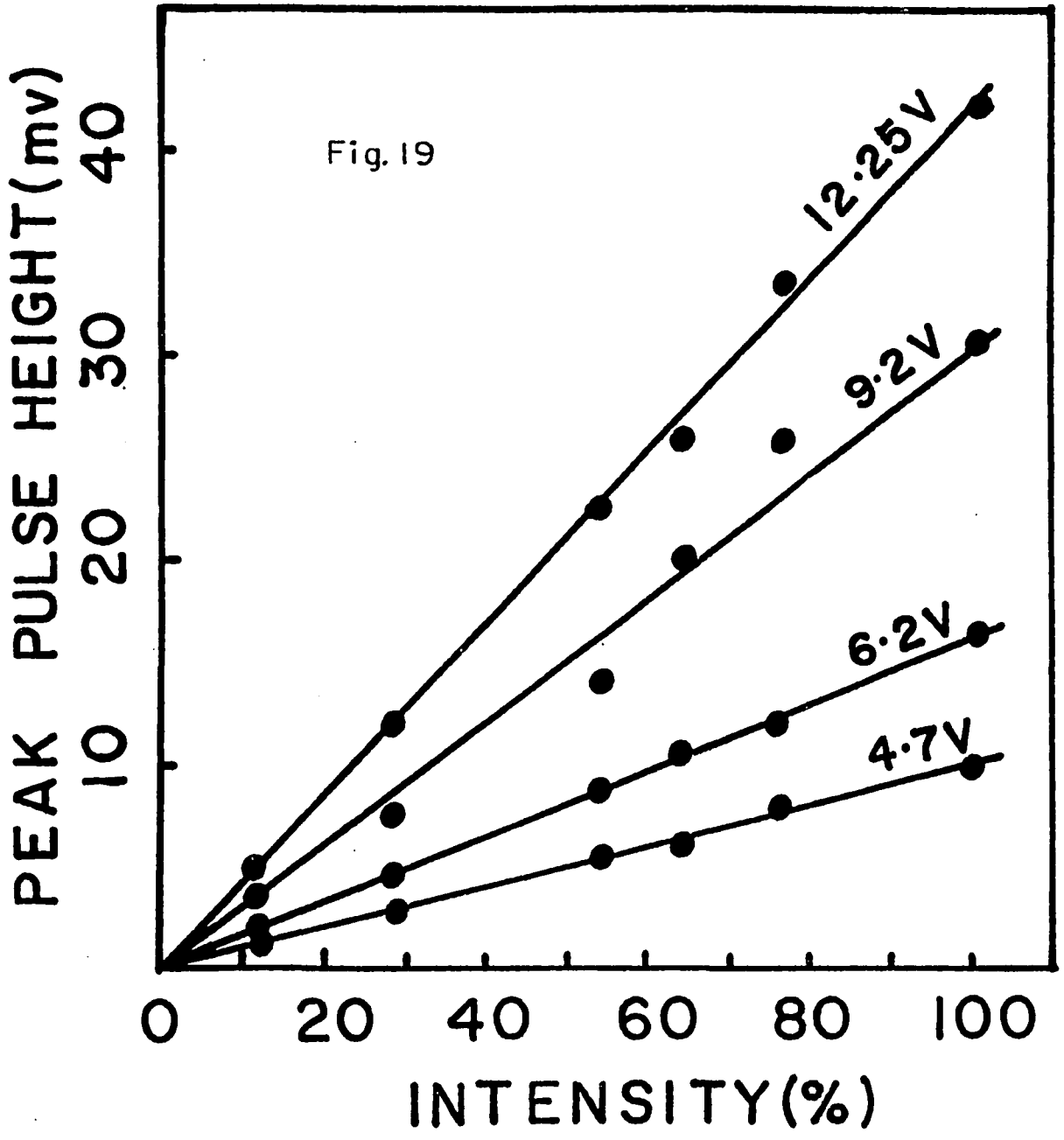
PEAK PULSE HEIGHT(mv)
10
20
30
40
0
20
40
60
80
100
INTENSITY(%)
12.25V
9.2V
6.2V
4.7V

Let us assume that the total pulse contains two charge components, the primary denoted by

$$q(t') = n_0 e E \mu t'/d \tag{47}$$

and a secondary component given by

$$a(t'') = (n_t e E \mu/d)(1-\exp[-t''/\tau_d]) \tag{48}$$

Where τ_d is a detrapping time, and all the traps characterized by this mean detrap time are supposed to exist at or near the initially irradiated surface. n_t is the equilibrium number of trapped holes in the surface region; it is understood that this surface trapping has reduced the size of the primary pulse by a proportionate amount. We may now write

$$q(t) = (E\mu e/d)(n_0 t' + n_t[1-\exp(-t''/\tau_d)]) \tag{49}$$

where $t' = 0$ at $t = t_0$, t_0 being the time after inception of the photolytic flash which is necessary to establish a steady state population of carriers, both free and trapped, and where $t'' = 0$ at $t = t_{tr}$. It is thereby supposed that surface detrapping becomes important only after the primary component has saturated. As a consequence of these assumptions

$$a(t) = (E\mu e/d)(n_0[t=t_0] + n_t[1-\exp-(t-t_{tr})/\tau_d]) \tag{50}$$

For $t_0 < t \leq t_{tr}$ we find $a(t) = E\mu et/d$, which is the behavior shown in Fig. 14. For $t > t_{tr}$, and such that $(t-t_{tr}) \geq \tau_d$ we find

$$q(t) = \text{constant} + n_t \ln t \tag{51}$$

A plot of v(t) vs. ln t is given in Fig. 20, wherein it is seen that linearity obtains, and that $t-t_{tr}$ is of the order of or slightly greater than τ_d. The break-time, t_S, in the ln t plot corresponds to the time of collection of the detrapped carriers, and if it be assumed to represent the saturation time then its dependence on voltage should generate a mobility and its dependence on temperature a surface trap depth.

Fig. 20. Photocurrent pulses in anthracene - cell XXII. The log t dependence of v(t) at $t \geq t_{tr}$ is indicated by regions of linearity. The break from linearity at longer times is indicated by an arrow and designated t_s. Irradiation was through filter C. S. 7 - 60.

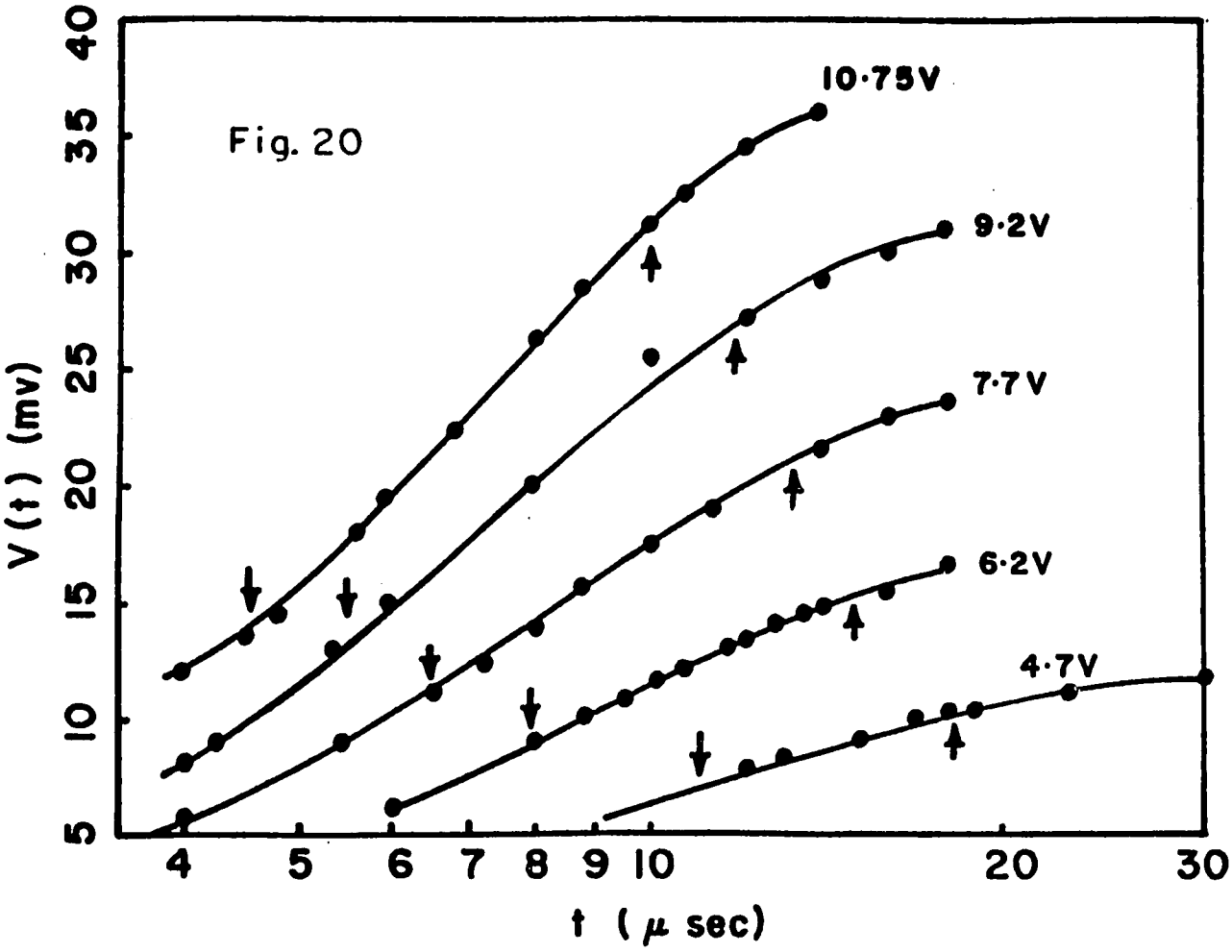
Fig. 20
10·75V
9·2V
7·7V
6·2V
4·7V
V(t) (mv)
5
10
15
20
25
30
35
40
4
5
6
7
8
9
10
20
30
t (μ sec)

The voltage dependence of t_s is shown in Fig. 21. The slope of the straight line obtained yields a value of 0.9 $cm^2/v.$ sec for the hole mobility, in good agreement with the values of Tables VI and VII. A plot of ln t_s vs. 1/T is given in Fig. 22. It is seen that t_s, in contrast to the transit time t_{tr}, decreases as the temperature increases. t_s is related to ΔE, the trap depth of shallow traps by the equation given by Michel.[12]

$$t_s = [\rho d T^{-1/2})/(\mu_0 \nu_0 V \tau_1)] \exp(\Delta E/kT) + t_1 \qquad (52)$$

where ρ = total distance travelled by holes in the region containing shallow traps, $\mu_0 = \mu/T^{-3/2}$, $\nu_0 = \nu T^2$ where ν is the attempt frequency, τ_1 - average time a hole spends in the valence band, ΔE = shallow trap depth, t_1 = flash duration. This in conjunction with Fig. 10, yields a value of 0.045 ev for the trap depth.

The above interpretation, while internally consistent and to some extent validated by the results of experiment based thereon, is not necessarily correct. It is entirely possible that the apparent poor integration of the pulses, if not due to the postulated detrapping, may arise from a decrease of the RC time constant. The combined capacitance of the output circuit, which consists primarily of the crystal capacitance, may decrease if a double-layer type of space charge is present at the surface of the crystal. The capacitance associated with such a double layer will vary inversely as some function of voltage, and also with the charge density of the space charge layer.

C-8. Properties of Electrons

Only very limited references are available describing the transport properties of negative charge carriers in organic crystals. LeBlanc gives a value of 0.54 $cm^2/v.sec$ for the mobility of electrons in anthracene.[13] In the present work, owing to the very small photocurrents ob-

---

[12] A. Michel, op. cit., vol. 121, p. 968.

[13] O. H. LeBlanc, op. cit., vol. 33, p. 626.

Fig. 21. Reciprocal t_s vs. applied voltage - cell XXII. Mobility, as determined from slope is 0.9 $cm^2/v.sec$.

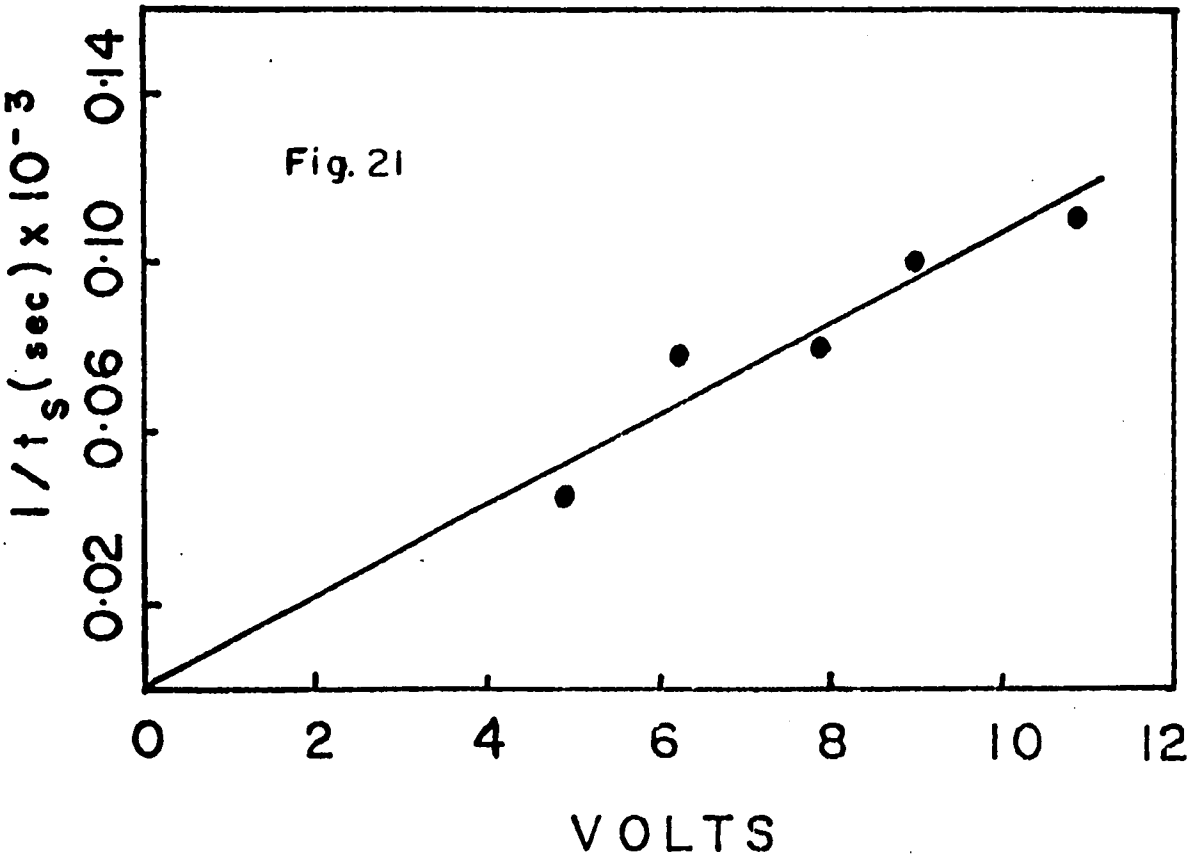
Fig. 21
$1/t_s$ (sec) x 10^{-3}
0·02
0·06
0·10
0·14
0
2
4
6
8
10
12
VOLTS

Fig. 22. Log t_s *vs.* 1/T for anthracene - cell XIII. The observed surface trap depth is 0.045 ev.

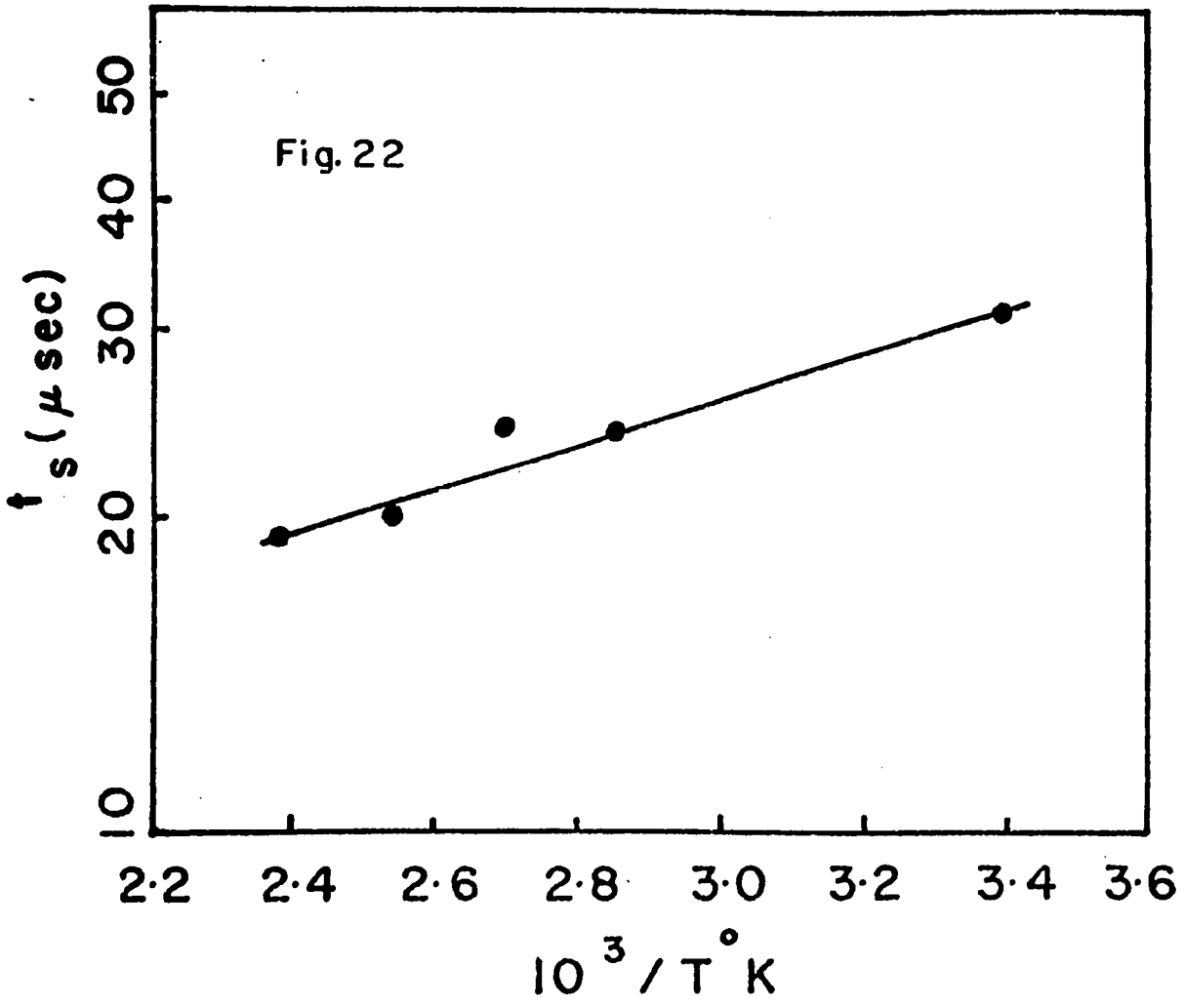
Fig. 22
t_s (μ sec)
10
20
30
40
50
2·2
2·4
2·6
2·8
3·0
3·2
3·4
3·6
$10^3 / T^\circ K$

served and their erratic nature, it was practically impossible to get meaningful transit times. However, a rough estimate turned out to be 0.37 $cm^2/v.sec$ at an applied voltage of 47 volts in cell XXII. Using equation (50) the lifetime was calculated as 7.3×10^{-6} sec which would yield a value of 2.6×10^{-7} $cm^2/v.$ for Schubweg. It is indicated then that hole lifetime and Schubweg are considerably larger than those of the electron.

C-9. High Voltage Effects

The anomalous non-Hecht behavior is evident from the effect of applied field on photocurrent. Typical examples are given in Figs. 23 and 24. In cells having thickness of the order of 15μ - 40μ the pulse height varied linearly with voltage in moderately low field regions and saturated or showed such a tendency at high fields (see Fig. 23). In thicker cells (45μ - 100μ) the trend was mainly super-linear. (See Fig. 24). Saturation in thicker cells could not be observed due to electric breakdown. In thinner crystals, where saturation was achieved, it was not possible to fit the data to Hecht's equation without taking values of μ an order of magnitude less than the values shown in Table VI. The generally observed exponent of the voltage in the log v_s vs. log V plots ranges from 1.2 - 1.6. This may be due to either the effect of field on quantum efficiency or on the rate of recombination at the surface as suggested by LeBlanc.[14]

It is appropriate to emphasize that non-Hecht behavior of pulse height with field is by no means uncommon. Michel[15] who has observed a similar behavior for silver chloride under pulsed x-ray irradiation has attributed this to a thin surface region near the illuminated electrode limiting the number of charge carriers entering the bulk. Similarly, surface imperfections have been shown to affect the transient

---

[14] Ibid.

[15] Michel, op. cit.

Fig. 23. Peak pulse height *vs.* voltage: A is cell II with d = 25.6μ and B is cell VIII with d = 20.6μ. Both cells were irradiated through the positive electrode. Pulses are typically *non*-Hecht, even though they do exhibit saturation. With Hecht behavior, saturation should have occurred at much lower voltages.

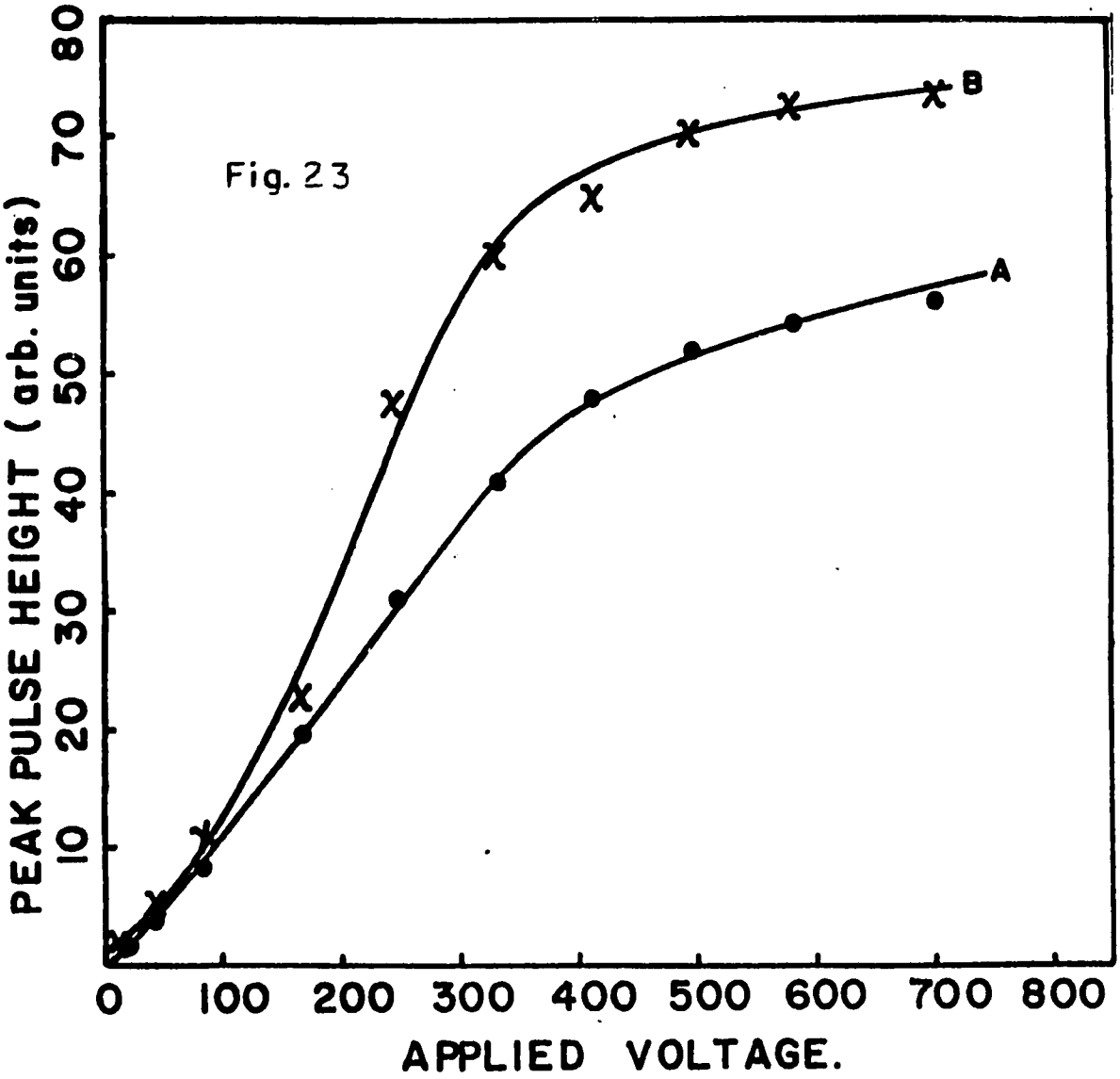
Fig. 23
PEAK PULSE HEIGHT (arb. units)
10
20
30
40
50
60
70
80
0
100
200
300
400
500
600
700
800
APPLIED VOLTAGE.
A
B

Fig. 24. Peak pulse height *vs.* voltage for anthracene - cell XVII with d = 60μ. Saturation is not observed, nor is an approach to it indicated.

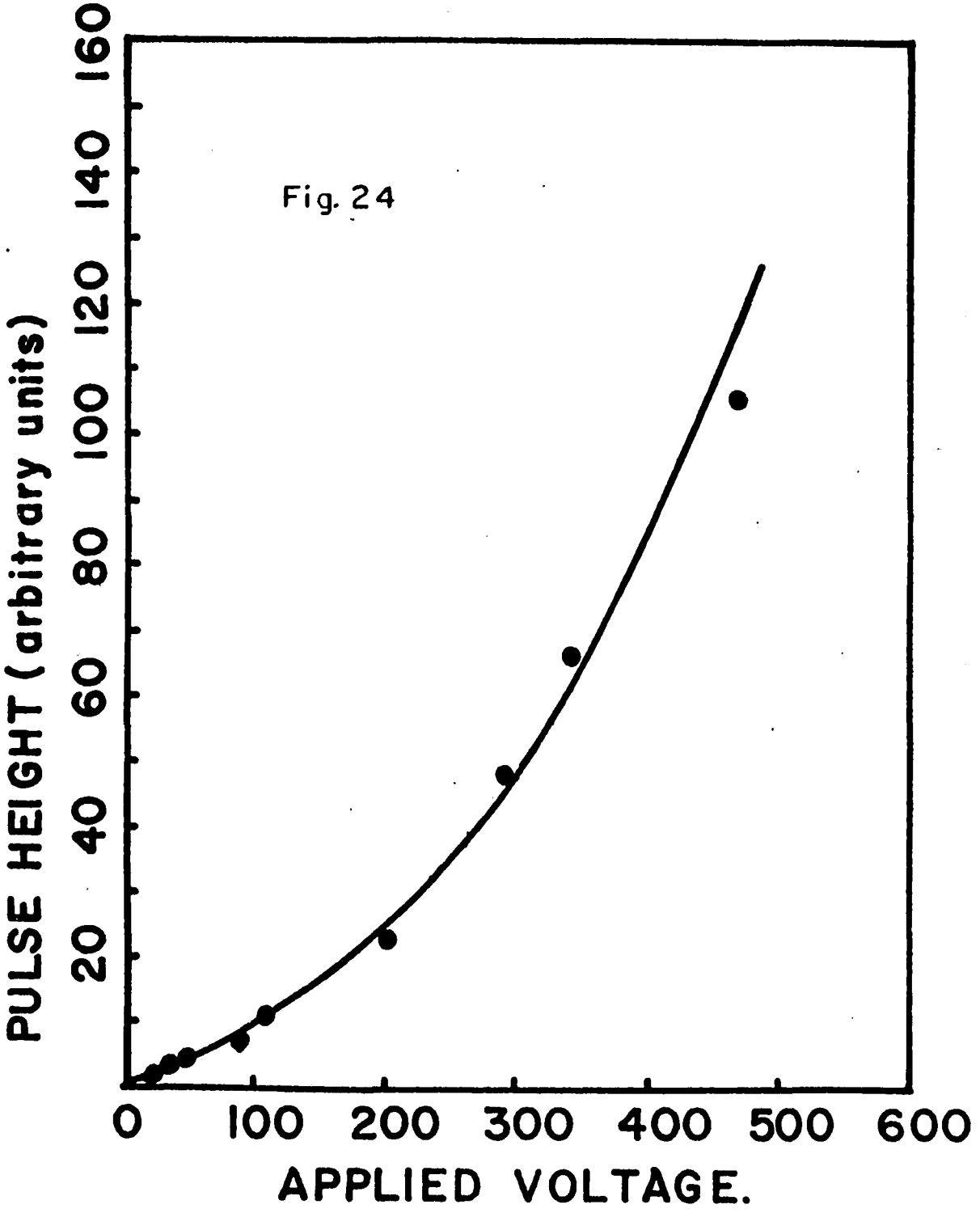
PULSE HEIGHT (arbitrary units)
20
40
60
80
100
120
140
160
0
100
200
300
400
500
600
APPLIED VOLTAGE.

Fig. 24

currents as in the case of experiments by Hoesterey.[16]

While we cannot formulate a unique or correct interpretation of this superlinearity we can hazard a few conjectures. Let us suppose that at the surface layer there exists a region where considerable recombination occurs. If we suppose that this recombination process is kinetically dominant, then the observed linearity of pulse height with incident photon density of Fig. 19 forces us to conclude that the carrier generative process at the surface is biphotonic. Kepler and Merrifield have recently conjectured similarly.[17] With these assumptions, the extent of recombination which will occur in the surface layer will be a function of the time which the two incipiently generated charge layers spend in contact with each other. Since the separation velocity of the two layers must be some function of the field strength, it is indicated that a larger hole pulse will be injected into bulk at larger voltages. The velocity of separation should lie between a $V^{1/2}$ and V dependence, and consequently $n_0 \propto V^x$, where $x < 1$. Since $q \propto n_0 V$ in the linear Hecht region, it is indicated that a V^{1+x} dependence could result. The observed value of x ranges from 0.2 to 0.6.

On the other hand we could assume that a rectification barrier caused by surface states is set up and that the crystal behaves as a typical p-n junction. The forward current given by $J = A[\exp(eV_0/kT)-1]$, V_0 being the voltage applied across the junction, might then be expected to show a linear rise when V_0 is large positive. The pulse height behavior of tetraphenylbutadiene shows full conformity to this type of behavior over the full range of V_0, both positive and negative. For anthracene, on the other hand, the negative pulses were erratic and irreproducible and the behavior with negative bias could not be followed very accurately; the positive pulses provided no evidence contrary to a p-n junction behavior, nor any significant evidence in its favor. We must conclude then that this latter interpretation is of

---

[16] D. C. Hoesterey, J. Chem. Phys., 36, 557 (1962)

17R. G. Kepler and R. E. Merrifield, J. Chem. Phys., 40, 1173 (1964).

importance only by correspondence with the tetraphenylbutadiene results and because of the superlinearity exhibited by anthracene itself. On the other hand the superlinearity observed may be due to the fact that the space charge fields set up by holes are not entirely negligible. This space charge may arise from both the moving holes and those in traps. However, we do not have any experimental evidence to show that space charge injection takes place using SnO_2 electrodes.

C-10. Quantum Efficiency

Theoretically quantum efficiency is calculated by studying the saturation region where it can be expected that all the charge carriers produced are pulled through the crystal. Unfortunately, the non-Hecht behavior restricts the use of pulse height data for such an evaluation. However, a rough estimate of η, the quantum efficiency per incident photon may be obtained by adopting an extrapolation approximation given by Wild and Brown.[18] This procedure involves the plotting of Q, the total charge induced as a function of applied electric field E, and then extrapolating the low field region as though there were no collection effects. In computing η the following equation is then utilized:

$$\eta\omega = (Qd^2)/(N_0eV) \qquad (53)$$

where N_0 is the total number of incident photons. From the slope of this line $\eta\omega$ is calculated. Fig. 25 gives such a calculation. Assuming $\omega = 5.4 \times 10^{-5} cm^2/v.$ one gets for η a value of 1.16×10^{-4} for cell XXII. For cell XVII, the value was 2.1×10^{-4}.

There is good correspondence between the above value of $\eta 400m\mu$ and the one (10^{-4}) reported by Carswell and Lyons.[19] However, as it has not been possible to obtain an absolute value for $\eta 402m\mu$ the present data can only be thought of as giving the order of magnitude of this parameter.

---

[18] R. L. Wild and F. C. Brown, Phys. Rev., 121, 1296 (1961).

[19] D. J. Carswell and L. E. Lyons, J. Chem. Soc., 1734 (1955).

Fig. 25. $(Q/N_0e)x10^{+4}$ *vs.* applied voltage for anthracene - cell XXII. Excitation wavelength was 402 mμ. Limiting slope gives $\eta\omega_0/d^2$ whence η is found to be $\sim 10^{-4}$.

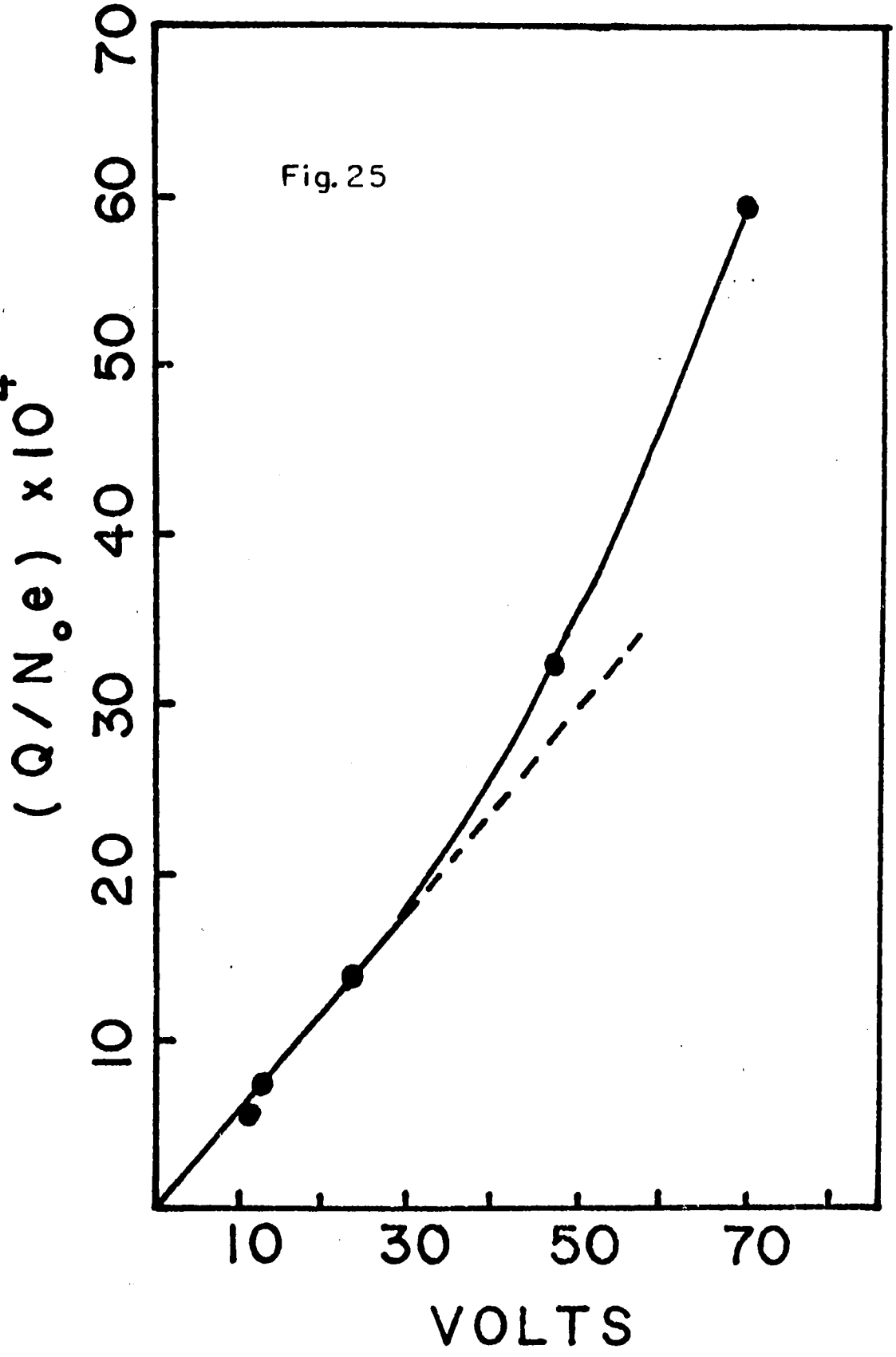
Fig. 25
70
60
50
40
30
20
10
$(Q/N_o e) \times 10^4$
10
30
50
70
VOLTS

C-11. Mobility Data For Various Organic Molecules

In the present work the mobility measurements were also done for tetraphenylbutadiene, stilbene and m-terphenyl. The results are given in Table IX.

TABLE IX

Mobility of Holes in Organic Crystals.

Compound	μ_+ (cm^2/V.sec)
Tetraphenylbutadiene	2.3×10^{-2}
m-terphenyl*	$\sim 10^{-5}$
stilbene*	$\sim 10^{-3}$

*) High field data.

CHAPTER V

CONCLUSIONS

The work reported here was undertaken in an effort to establish the nature of charge carrier generation by optical excitation. This objective has not been achieved. However, a number of conclusions is possible and these are serialized below:

1. The photogenerative process is fast; it is certainly less than 0.6 microseconds.

2. The photocurrent is linear with light intensity when the exciting light is polychromatic and is strongly absorbed in the crystal. This linear dependence was observed for both pulsed and steady illumination.

3. The photocurrent is linear with light intensity when a monochromatic and strongly absorbed light is used for excitation.

4. Under steady illumination with monochromatic and very weakly absorbed radiation, the photocurrent varies sublinearly with light intensity.

5. The dependence of the photocurrent on light intensity is dependent also upon the intensity of the applied electric field. The general tendency is for the photocurrent to vary with higher powers of light intensity for higher intensities of the applied electric field. In no case, however, was the photocurrent observed to vary as the square of light intensity. It may be concluded that there is at least one kinetically important process which is field dependent; this may possibly be a rate of detrapping which increases with the electric field or a rate of recombination which decreases with increasing electric field.

6. The conclusion that may be made from the analysis of the photoconduction action spectra of anthracene, rubrene and tetraphenylbutadiene is that the rate of recombination at the surface is not negligible compared with the rate of recombination in the bulk of the crystal.

7. Items 1, 2, 3, 5, and 6 seem to indicate that charge carrier generation by strongly absorbed light may be biphotonic.

8. There is a high density of trapping centers 0.39 ev. below the conducting levels in m-terphenyl. The trapping cross-section is of the order of 1.5×10^{-18} cm^2; the attempt-to-escape frequency is of the order of 3.8×10^{8}/sec and the mean free time between trapping is of the order of 4×10^{-8} sec.

9. Fairly deep trapping states (0.6 ev. below the conducting levels) with a density comparable to that of m-terphenyl were also found in anthracene sandwich cells.

10. The very low measured value of mobility in m-terphenyl is probably a consequence of trap modulation of the drift mobility. A non-trap-modulated value of mobility was calculated and found to be of the order of 4.5 cm^2/V sec.

11. The mobility of holes in a direction perpendicular to the 001 face of anthracene is 0.45 - 1.5 $cm^2/v.$ sec.

12. Hole mobility in anthracene varies at T^{-n}, where n ranges from 1.73 to 2.30. Hole mobility is apparently limited primarily by scattering due to the acoustic branch of the lattice vibration spectrum.

13. Hole mean free lifetime is of the order of 10^{-4} sec in anthracene.

14. The dependence of hole population on temperature in anthracene is exponential, the activation energy being 0.14 ev. The closeness of this value to that observed in DC measurements (0.17 ev) perhaps indicates that such DC measurements do indeed measure a true carrier population activation energy.

15. Electron mobility in a direction perpendicular to the 001 face of anthracene is approximately 0.4 $cm^2/v.sec.$

16. The pulse shape is linear at short times ($t < t_{tr}$), but exhibits an abnormally large component which does not saturate until times of the order of $6t_{tr}$. It has been shown that the larger part of this secondary pulse component varies as lnt in accord with predictions of a model which analyzes this component as due to release of carriers from traps.

17. The break in the ln t linearity which occurs at t_s can be used in conjunction with voltage variation to define a mobility which accords well with that of 16 above. The t_s *vs.* T dependence defines a surface trap depth for holes of 0.04 ev.

18. Zero-field quantum efficiency at 402 mμ when the anthracene crystal is in contact with the SnO_2 electrodes is $\sim 10^{-4}$.

19. Further work is necessary to ascertain the nature of the trapping and recombination centers and their respective importance in the kinetics of photoconduction. The experimental results for *m*-terphenyl and anthracene indicate that the charge carriers are scattered mainly by acoustical phonons. This needs further substantiation. The problem of photogeneration of carriers calls for a detailed investigation of the electronic states of organic molecular crystals.

SELECTED BIBLIOGRAPHY

Bardeen, J., Phys. Rev., 71, 717 (1947).

Bardeen, J. and Brattain, W. H., Ibid., 75, 1208 (1949).

Bube, R. H., "Photoconductivity of Solids:, John Wiley and Sons, Inc., New York (1960).

Bube, R. H., Phys. Rev., 106, 703 (1957).

Carswell, D. J. and Lyons, L. E., J. Chem. Soc., 1735 (1955).

Child, C. D., Phys. Rev., 32, 492 (1911).

Compton, D. M. J., Schneider, W. G. and Waddington, T. C., J. Chem. Phys. 27, 160 (1957).

Craig, D. P. and Hobbins, P. C., J. Chem. Soc., 2309 (1955).

Dekker, A. J., "Solid State Physics," Prentice-Hall, Englewood Cliffs, N. J. (1961).

Garlick, G. F. and Wilkins, M. H. F., Proc. Roy. Soc., 184A, 408 (1945).

Grossweiner, L, I., J. Appl. Phys., 24, 1306 (1953).

Hecht, K., Z. Physik, 77, 235 (1932).

Hoesterey, D. C., J. Chem. Phys., 36, 557 (1962).

Kepler, R. G., Phys. Rev., 119, 1226 (1960).

Kepler, R. G. and Merrifield, R. E., J. Chem. Phys., 40, 1173 (1964).

Kleinerman, M., Azarraga, L. and McGlynn, S. P., Ibid., 37, 1825 (1962).

Kommandeur, J., Ph. D. Dissertation, University of Amsterdam, February 19, 1958.

Landau, L., Physik. Z. Sowjetunion, 3, 664 (1933).

Langmuir, I., Phys. Rev., 2, 450 (1913).

LeBlanc, O. H. (Jr.), J. Chem. Phys., 33, 626 (1960).

Lyons, L. E., J. Chem. Phys., 23, 220 (1955).

Mark, P. and Helfrich, W., J. Appl. Phys., 33, 205 (1962).

Michel, A. E., Phys. Rev., 121, 968 (1961).

Mott, N. F., Proc. Roy. Soc., 171A, 27 (1939).

Mott, N. F. and Gurney, R. W., "Electronic Processes in Ionic Crystals," Oxford (1948).

Northrop, D. C. and Simpson, O., Proc. Roy. Soc., 244A, 377 (1958).

Randall, J. T. and Wilkins, H. M. F., Ibid., 184A, 347, 366 (1945).

Rose, A., R. C. A. Rev., 12, 362 (1951).

Rose, A., Phys. Rev., 97, 1538 (1955).

Schottky, W., Z. Physik, 118, 539 (1942).

Shockley, W., Phys. Rev., 56, 317 (1939).

Shockley, W., "Electrons and Holes in Semiconductors", Van Nostrand, New York (1950).

Shockley, W., Bell Syst. Tech. J., 30, 990 (1951).

Shockley, W., Proc. I. R. E., 40, 1289 (1952).

Shockley, W. and Pearson, G. L., Phys. Rev., 74, 232 (1948).

Shockley, W. and Read, W. T., Ibid., 87, 835 (1952).

Smith, R. A., "Semiconductors", Cambridge University Press (1959).

Van Heyningen, R. J. and Brown, F. C., Phys. Rev., 111, 462 (1958).

Wagner, K. W., Elec. Eng., 41, 1034 (1922).

Wild, R. L. and Brown, F. C., Phys. Rev., 121, 1296 (1961).

Yamakawa, K. A., Ibid., 82, 522 (1951).

Zener, C., Proc. Roy. Soc., 160A, 523 (1934).

VITA

Leo Villaraiz Azarraga was born in Roxas City, Philippines on February 1, 1933. He finished his elementary education from Loctugan Elementary School in 1948. He graduated from Feati University High School in Manila in 1952. In April, 1956, he graduated from the University of the Philippines with a B. S. degree in Chemistry. He worked with the Standard Vacuum Oil Company and was Instructor in Chemistry at the University of the Philippines, College of Agriculture before coming to the United States. He is presently a candidate for the degree of Doctor of Philosophy in Chemistry at the Louisiana State University.

GLOSSARY

α ..... absorption coefficient; proportional to

β ..... rate of heating

δ ..... diffusion length for holes

ϵ ..... dielectric constant

η ..... quantum efficiency

θ ..... fraction of free space-charge

λ ..... wavelength

μ ..... charge carrier mobility

μ ..... when written as mμ or with a number such as 45μ, means micron

μ_+ ..... hole mobility

μ_- ..... electron mobility

ν ..... attempt-to-escape frequency

ξ ..... a proportionality factor related to η

σ or σ_t ..... trapping cross-section

τ or τ_0 ..... charge carrier lifetime

υ ..... velocity of sound

Φ ..... fraction of hot electrons in the injected space charge

ω ..... range of the charge carrier

ω_o ..... range of the charge carrier per unit electric field

b ..... thickness of the illuminated layer

C ..... capacitance

C_T ..... total capacitance

d ..... thickness of the crystal

E ..... electric field

E_t ..... trap depth

e (without exponent) .... electronic charge

e (with exponent) ..... base of natural logarithm

I ..... light intensity

J ..... current

J_d ..... dark current

J_p ..... photocurrent

J_{p+} ..... photocurrent when the illuminated side is positive

J_{p-} ..... photocurrent when the illuminated side is negative

L ..... rate of photogeneration

N_o ..... number of incident photons per flash per cm^2

N_t ..... trapping state density

N_v ..... density of states in the valence band

N_c ..... density of states in the conduction band

n ..... charge carrier density

n^o ..... density of charge carriers in the dark at thermal equilibrium

Q ..... total induced charge

q(t) ..... time-dependent induced charge

s ..... surface recombination velocity

T ..... absolute temperature

t ..... time

t_S ..... saturation time

t_{tr} ..... transit time

V ..... voltage

V_s ..... saturation voltage

v(t) ..... time-dependent induced voltage

EXAMINATION AND THESIS REPORT

Candidate: Leo Villaraiz Azarraga

Major Field: Chemistry

Title of Thesis: Photoconductivity of Non-Ionic Crystalline Organic Substances

Approved:

S. P. McGlynn
Major Professor and Chairman

Max Goodrich
Dean of the Graduate School

EXAMINING COMMITTEE:

J. L. E. Ericsson

D. W. Pratt

Robert V. Naumann

Nicola Nicolaides

Date of Examination:

July 27, 1964